BIOPHYSICAL CHARACTERIZATION OF HCV Q65H NS5B AND EIF4B : PROTEIN – NUCLEIC ACID INTERACTIONS

By

SHEMAILA SULTANA

A dissertation submitted to the Graduate Faculty in Biochemistry in partial fulfillment of the requirements for the degree of Doctor of Philosophy,

The City University of New York

2010

The manuscript has been read and accepted for the Graduate Faculty in Biochemistry in satisfaction of the dissertation requirement for the degree of Doctor of Philosophy.

Prof. Dixie J. Goss

Date

Chair of Examining Committee

Prof. Edward J. Kennelly

Date

Executive Officer

Prof. Frida Kleiman

Prof. Gary Quigley

Prof. Lesley Davenport

Prof. Susan Rotenberg

Supervisory Committee

THE CITY UNIVERSITY OF NEW YORK

Abstract

Biophysical Characterization Of HCV Q65H NS5B and eIF4B : Protein – Nucleic Acid Interactions

By

Shemaila Sultana

Adviser : Professor Dixie J. Goss

Hepatitis C Virus (HCV) infection is one of the most common chronic blood borne infections. The mechanism underlying persistence of HCV infections are not well understood. Mutation of Gln65His (Q65H), which develops in the NS5B dependent RNA polymerase (RdRp) during chronic infection, has 1.8 fold enhanced invitro RdRp activity, may have major implications in the efficiency of HCV RNA replication and viral persistence. The reason for this increase in activity is not well understood (Virology 2003 Dec 5; 317(1):65-72). We used endogenous tryptophan fluorescence to characterize the interactions of Q65H protein with GTP, GDP, Mg^{2+} and a 19mer RNA template. The Q65H protein exhibits 3 fold lower Kd (11.6 ± 1.2 μM) than wildtype (36.8 ± 1.0 μM) for GTP, whereas the Kd values of the mutant for $MgCl_2$ and 19 mer RNA template were similar to wildtype protein. Thermodynamic studies on the binding reaction of the

Q65H variant were also performed to provide details of the energetic and entropic characteristics.

The second part of this study involved interaction of eIF4B with zinc. eIF4B promotes RNA dependent ATP hydrolysis and ATP dependent RNA helicase activity of eIF4A and eIF4F. It has recently been reported that eIF4B also organizes assembly of the RNA, eIFiso4G, eIF4A, and poly-(A) binding protein and that zinc enhances the RNA binding and interaction with PABP. We previously reported that zinc binds tightly with eIF4B with a K_d of 19.7 ± 1.6 nM (J Biol Chem. 2008 Dec 26; 283(52):36140–53). The K_d of binding of eIF4B with 20mer poly (A) RNA is 77 ± 7 nM and in presence of zinc is reduced down to 45 ± 3 nM. Circular dichroism showed that addition of zinc resulted in a more than 50% decrease in alpha content of the eIF4B protein. To better understand the role of eIF4B in the selection of RNA, we also studied the interaction of eIF4B with structurally different RNAs and the effect eIF4A on this interaction using fluorescence anisotropy. This overall study on eIF4B helps towards the better understanding of basic translation initiation machinery and some of its regulators.

To my parents, for all the years of love, nurturing, protection and care.

Acknowledgements

I take this opportunity to express my sincere thanks and gratitude to my mentor Prof. Dixie Goss who painstakingly introduced me to the field of biophysics and nurtured in me the ability for independent work, her magnanimous generosity and unflagging interest helped me in all my endeavors.

I am grateful to Prof. John Trujillo for his valuable suggestions and guidance from time to time and for inspiring the lab with his friendly and helping attitude.

I would like to thank Prof. Lesley Davenport, the former executive officer of Biochemistry program, CUNY (also member of my doctoral committee) and current executive officer Prof. Edward Kenelly for their active support and making my transition easy and smooth as a graduate student.

My thanks to doctoral committee members, Prof. Frida Kleiman, Prof. Susan Rotenberg and Prof. Gary Quigley for being a part of my doctoral committee and for offering suggestions and gauging the progress at every stage. Their scientific outlook and constructive criticism has always helped me device analytical and scientific approach to the problem. I would like to thank Prof. Klaus Grohmann for the help and support he provided during my initial years in the graduate program. Thanks to Ms. Judy Li (assistant Biochemistry program Officer), Ms. Nala Fernando and Ms. Mirela Settenhofer (Dept. of Chemistry, Hunter College) for all the help with paper work throughout my stay at CUNY.

I am grateful to our collaborator Prof. Curt H. Hagedorn for providing the purified proteins for HCV project and Prof. Daniel R. Gallie for providing the eIF4B constructs and for their valuable suggestions from time to time.

I would like to thank my colleagues Sumeyra, Bidisha and Sohani who always inspired me with their gregarious and friendly attitude and helped me soothe my moments of anxiety. Pragya, Pooja and Angelika had been more than batch mates, whose company made the coursework and graduate study a fun time.

It is always a pleasure having Dr. Mateen, Jia Ma and Artem around for scientific trouble shooting and the help extended by them is greatly acknowledged. My predecessors and former members of the lab Dr. Diana, Dr. Sibnath, Dr. Anamika, Dr. Ozgur and Dr. Hassan who are a driving force and path bearers for the young talents from the group.

It is a rare and special thing to get an extremely supportive and encouraging in-laws (Papa & Mummy), who have always been there at every stage of our lives and their genuine emotions and support is always appreciated.

I would like to thank my three brothers (Suhail, Athar and Khursheed) and their families for their unconditional support. To the very special aunts and their families Ms. Ghousia Sultana, Mrs Sabiha Khan and Mrs. Naheed Mashood who have always been there for me at every step of my upbringing and always guided

me with their inspirational talks and profound love at all times and in moments of need.

My dearest papa and mummy for all the years of love, nurturing protection and care. They have always been there at every stage of my life and their genuine love, continuous encouragement and inspirations shall always remain indelible in my heart and life.

Words can never summarize my feelings of love and emotions for my adorable and sweetest daughter Mysha who is almost as old today as the duration of my thesis work. Her delightful distractions and understanding always inspired me while at work and completing this thesis.

Lastly to my understanding and cooperative husband Javed, in whom I found my best of best friend, who always stands like pillar and is a motivating force for a much stronger will power. Without his love and unconditional support this thesis wouldn’t have been possible.

Table of Contents

List of Tables

List of Figures

List of Abbreviation

HCV	Hepatitis C Virus
NHANES	National Health and Nutrition Examination survey
NS5B	Non Structural 5B
RdRp	RNA dependent RNA polymerase
Gln	Glutamine
His	Histidine
GTP	Guanosine-5'-triphosphate
GDP	Guanosine diphosphate
eIF	Eukaryotic Initiation Factor
kDa	Kilo Dalton
PABP	Poly (A) Binding Protein
CD	Circular Dichroism
IPTG	Isopropyl β-D-thiogalactopyranoside
HEPES	4-(2-hydroxyethyl)-1-piperazineethanesulfonic acid
EDTA	Ethylenediaminetetraacetic Acid
DTT	Dithiothreitol
RRM	RNA Recognition Motif
nt	Nucleotide
bp	Basepair
LB	Luria-Bertani Media
SDS-PAGE	Sodium Dodecyl Sulfate Polyacrylamide Gel Electrophoresis

Chapter 1: Hepatitis C Virus Q65H NS5B Mutant Protein and its Ligands

1.1. Introduction

1.1.1. Hepatitis C Virus

Hepatitis C Virus (HCV) is a single stranded positive sense RNA virus, belonging to the *Flaviviridae* class of virus family [5]. HCV infection is one of the most common chronic blood borne infections, affecting more than 3.9 million (1.8%) people in the US itself according to the National Health and Nutrition Examination survey (NHANES) of 1988-1994, and more than 170 million people worldwide [6, 7]. Of those in the US, 2.7 million (80%) of infected individuals with acute HCV infection develop chronic hepatitis, while 20% of that develop cirrhosis and 1-5% develop hepatocellular carcinoma [5, 8-11]. There is no effective means to fight HCV infection [12] and there is an urgent need to study and develop various drug targets that are susceptible in this pathogen. The mechanism underlying the chronicity of HCV infection is also not well understood. Several viral host interactions which affect the interferon regulated pathway or the immune system might be involved in the chronicity of HVC infection [1, 13]. Mutations in the viral genome are another well studied area related to chronicity. Mutations accumulate over the course of time in the HCV genome during viral replication because of the lack of a proof reading function in its RNA dependent RNA polymerases [14], a characteristic of RNA viruses. This results in genetic variability in the hepatitis C virus genome. This genetic evolution might be the reason for the easy escape of HCV from the host immune system [15]. This

makes these mutations an interesting target of study to better understand HCV infection and its chronicity.

1.2.1. **Non-Structural Protein 5B and its Mutants**

NS5B (non structural 5B), a 66 kDa protein is a key replicative enzyme of the Hepatitis C virus. NS5B is derived from the C terminal end of the viral polyprotein [16-21]. A characteristic Gly-Asp-Asp (GDD) motif is present in this protein, common in RNA dependent RNA polymerases, indicating that NS5B belongs to this family of enzymes [16, 17] and is involved in replication of the viral genome. The polymerase activity has been confirmed for recombinant NS5B protein expressed in both insect cells and *Escherichia coli* [12, 17-20, 22-31]. The characteristic GDD domain binds with Mg^{2+} ions that are required by polymerases for their activity [16, 21].

The NS5B polymerase of HCV contains a classic right hand shape with fingers, palm and thumb subdomains similar to other polymerases [32, 33] (figure.1). The HCV NS5B has a more compact shape as compared to other polymerases, and the active site of the enzyme, which is accessible to RNA template and NTP substrate, is completely surrounded by fingers, thumb and palm subdomains [34, 35]. The palm domain contains two metal ion catalytic centers that are

conserved in most polymerases and are required during polymerase function [35].

There are reports that mutations in the HCV NS5B polymerase that occur during infection may affect RNA dependent RNA polymerase (RdRp) activity [1]. These mutations in the viral genome occur spontaneously during viral replication as a result of the high rate of virion production and lack of proof reading function in HCV polymerase. One such mutation from Gln to His residue at position 65 in the finger domain [1], which develops in the coding region of NS5B during chronic infection, may have major implication in the efficiency of HCV RNA replication and viral persistence. It has been reported that a mutation Gln 65 His (Q65H) residue enhances *in vitro* RdRp activity by as much as 1.8 fold [1] and the reason for this increase in activity is not understood. The location of Gln 65 in NS5B crystal structure is close to the Arg 345 residue which stimulates RdRp activity 2-3 fold when mutated to Lys [1].

In this study we characterize the interactions of the Q65H NS5B mutant protein with GTP, GDP, Mg^{2+} and a 19mer RNA template by utilizing endogenous tryptophan fluorescence. This is the first report of how the mutation affects the binding properties of NS5B to its ligands, template and metal ion.

Figure 1. ***Location of the mutations in the HCV NS5B polymerase [1]. A ribbon diagram of NS5B (finger, palm, and thumb domains colored red, yellow, and blue, respectively) with circled Gln-65 residue.***

1.2.2. **Fluorescence Spectroscopy**

Fluorescence spectroscopy is a very sensitive technique used to study various biochemical and biophysical problems. The first step involves excitation of the fluorophore to higher energy level (electronic singlet state (S_1')) by absorption of photon of energy using an energy source such as a xenon lamp. The excited state typically has a nano - second duration. In the excited state changes can take place in the conformation of the molecule and also, it has the possibility of multiple interactions with the surrounding molecular environment. The excited molecule partially dissipates some energy yielding relaxed singlet excited state (S_1)) which decays to the ground state (S_0) with the emission of light [36]. The energy released during this process produces emission spectra that are characteristic of a particular compound.

The emission spectrum is quite sensitive to changes within the environment and can be used to study and measure the changes within the molecule, its interaction to other components and the environment. In biological systems, the amino acids containing aromatic rings such as tryptophan, tyrosine or phenylalanine are used as intrinsic molecular probes to gain a better understanding of proteins and their interactions [4, 36].

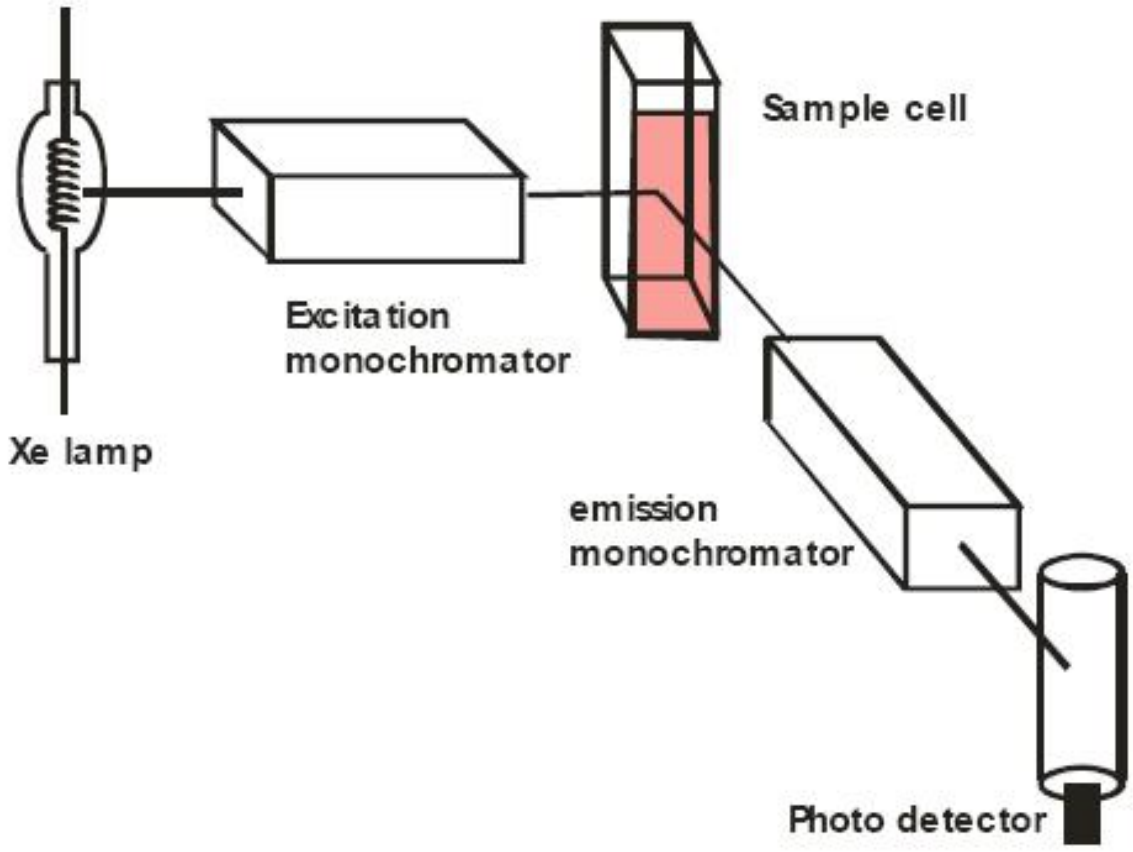

Figure 2 . ***A basic diagram of a spectrophotometer (Wikipedia).***

Experimental procedures

1.2.1. Materials:

We received the wild type and Q65H mutant hepatitis C virus non-structural protein 5B from our collaborator Prof. Curt H. Hagedorn, Gastroenterology Division, University of Utah, Salt Lake City, UT. 19nt RNA template named LE19 [37] was purchased from Dharmacon, Inc.

1.2.2. Fluorescence Measurements

Fluorescence measurements were carried out at 22 °C (unless otherwise noted) on a SPEX Fluorolog-τ-2 spectrofluorometer equipped with a high-intensity (450 W) xenon arc lamp. Excitation and emission slit widths of 2.0 and 3.0 mm were used, and a path length of 1.0 cm was employed. Experiments using NS5B Q65H were performed using an excitation wavelength of 280 nm to monitor the emission at 330 nm. The background emission was eliminated by subtracting the signal from buffer containing an appropriate quantity of substrate. Data were averages of three or more titrations. The binding buffer used for all fluorescence studies consisted of 50 mM Tris-HCl, 50 mM KOAc (pH 7.5). All chemicals were molecular biology grade. Binding experiments were performed using 150 nM NS5B Q65H mutant protein to which increasing amounts of GTP, GDP, Mg^{2+} were added individually in different experiments.

To study the template binding properties of the mutant protein experiments were done using 19nt RNA template named LE19 [37] alone and in combination with either GTP or Mg^{2+} ion with increasing amounts of RNA. The sequence of 19nt RNA template is 5' UGUUAUAAUUAUUGUAUAC 3'. This 19nt sequence is a derivative of 3' end of the minus-strand RNA of bovine viral diarrhea virus (BVDV). The three nucleotide unpaired initiation sequence in LE19 is predicted to form a simple stem-loop structure at the 3' end that directs initiation of *de-novo* RNA synthesis [37].

1.2.3. Data Treatment

The binding of ligands to the NS5B Q65H protein was determined by examining the florescence emission of a fixed concentration of protein and titrating with increasing concentrations of a given ligand in binding buffer. The equilibrium expression is:

$$K_d = [NS5B_{(Q65H)}][ligand] / [NS5B_{(Q65H)}.ligand] \qquad \text{(eq. 1)}$$

where K_d is the apparent dissociation equilibrium constant, $[NS5B_{(Q65H)}]$ is the concentration of the protein, $[NS5B_{(Q65H)}\cdot ligand]$ is the concentration of complexed protein, and [ligand] is the concentration of unbound ligand.

Further,

$$NS5B_{(Q65H)total} = [NS5B_{(Q65H)}] + [NS5B_{(Q65H)}.ligand] \quad \text{(eq. 2)}$$

And

$$[ligand_{total}] = [ligand] + [NS5B_{(Q65H)}.ligand] \quad \text{(eq. 3)}$$

So,

$$[NS5B_{(Q65H)}.ligand] = [ligand_{total}] - [ligand] = [NS5B_{(Q65H)total}] - [NS5B_{(Q65H)}] \quad \text{(eq. 4)}$$

We can write

$$[ligand] = [ligand_{total}] - [NS5B_{(Q65H)total}] + [NS5B_{(Q65H)}] \quad \text{(eq. 5)}$$

Therefore, from equation 1, 2 and 5

$$K_d = \frac{[NS5B_{(Q65H)}] \{ [ligand_{total}] - [NS5B_{(Q65H)total}] + [NS5B_{(Q65H)}] \}}{[NS5B_{(Q65H)total}] [NS5B_{(Q65H)}]} \quad \text{(eq. 6)}$$

We also know that the fraction of ligand bound to protein is related to the florescence measurement as follows

$$F_{\text{fraction bound}} = [F_{obs}] - [F_o] \;/\; [F\infty] - [F_o] = [NS5B_{(Q65H)}] / [NS5B_{(Q65H)total}] \quad \text{(eq. 7)}$$

Where $F_{[bound]}$ is the fraction of ligand bound to the protein, $F_{[obs]}$ is the observed fluorescence, $F_{[o]}$ is the fluorescence observed in absence of any ligand (that is the fluorescence of the protein), and $F\infty$ or $F_{[final]}$ is the fluorescence with the ligand when there is no more change in intensity observed.

So from equation 6 and 7 we can define that the proportion of ligand-bound protein is related to the measured fluorescence emission intensity by the following equation.

$$F_{[bound]} = (F_{[obs]}-F_{[o]})/\{[(F_{[final]}-F_{[obs]})(F_{[final]}/F_{[o]})]+(F_{[obs]}-F_{[o]})\} \quad \text{(eq.8)}$$

Once we calculate the fraction bound, we plot $F_{[bound]}$ versus the total ligand concentration and the resulting dissociation equilibrium constants were obtained by fitting the titration data to the equation

$$Y = ((N_{tot}+P_{tot}+K_d)-((N_{tot}+P_{tot}+K_d)^{2}-(4* N_{tot} * P_{tot}))^{0.5})/(2* P_{tot}) \quad \text{(eq.9)}$$

where N_{tot} [or $ligand_{total}$], P_{tot} [or $NS5B_{(Q65H)total}$], and K_d are the total concentrations of ligand, protein and the dissociation equilibrium constant, respectively. These calculations were performed using Kaleidograph 4 software. The values were confirmed by Graph Pad Prism 4.0 software, using its saturation binding equation. The number of binding sites was determined by fitting the data for one binding site and two binding site models of Graph Pad Prism 4.0. Scatchard analysis was performed using Graph Pad Prism 4.0 software.

1.2.4. Thermodynamics of binding

Thermodynamic parameters, ΔH (van't Hoff enthalpy), ΔS (entropy), and ΔG (free energy), were determined using the following equations [38]

$$\Delta G = -RT\ln K_a \qquad \text{(eq. 10)}$$

$$\ln K_a = -\Delta H/RT + \Delta S/R \qquad \text{(eq. 11)}$$

R and T are the universal gas constant and absolute temperature, respectively. K_a, the association equilibrium constant, was determined at four different temperatures 10, 15, 21 and 25 °C, respectively. ΔH and ΔS were determined from the slope and intercept of a plot of ln (K_a) vs 1/T. ΔG was determined from equation 10.

1.3. **Results**

1.3.1. Fluorescence titration of HCV NS5B Q65H mutant protein and wildtype protein with GTP

To determine the binding constants for the mutant and wildtype structural protein with its ligand, GTP, direct fluorescence studies were performed as shown in Figure 3. The K_d was calculated as described in Material and Methods. The binding of GTP with the NS5B protein resulted in a significant decrease in the emission fluorescence intensities as observed in earlier work for wild type protein [39]. This modification of intrinsic florescence of protein upon GTP binding was utilized in the present studies to calculate the K_d. The Q65H mutant exhibits a K_d of 11.6 ± 1.2 μM at 22°C. The value is six times lower than what is reported for the wild type NS5B protein i.e., 65 μM [39] and three times lower than the K_d for wildtype calculated by us thereby indicating that the mutant protein binds GTP more tightly than the wild type protein.

Thermodynamic studies on the binding reaction were carried out to provide a better understanding of the energetic and entropic characteristics of the binding reaction of wildtype and Q65H mutant protein with GTP. The dissociation equilibrium constant at different temperatures is shown in Table 2b. From the temperature dependence of these dissociation constants, the thermodynamic

parameters for mutant protein and wildtype protein with respect to GTP were calculated (Table 2a). Comparative study of mutant and wildtype protein was carried out only with respect to GTP and not with GDP, Mg^{2+} ion and RNA template because of limitation of availability of wildtype protein. Figure 4 shows the van't Hoff plot based on GTP binding to wildtype and mutant protein; the values of ΔS and ΔH were obtained from the intercept and slope, respectively (correlation coefficient>0.95). Figure 3 shows a titration curve and the Scatchard plot. The linearity of the Scatchard plot demonstrates that there is one binding site for the GTP in the NS5B protein. Further the Kd obtained from the Scatchard plot corresponded to the K_d obtained from fitting the titration curves by KaleidaGraph 4.0 as discussed in Material and Methods.

Complex	Kd (μM)
NS5B Q65H +GTP	11.6±1.2
NS5B wildtype +GTP	36.8 ± 1.0
NS5B wildtype +GTP	65 μM (*J Biol Chem 2003:* 278(6), 3868-38751)

Table 1*. Equilibrium dissociation constants for the interaction of HCV NS5B Q65H mutant and wild type NS5B with GTP.*

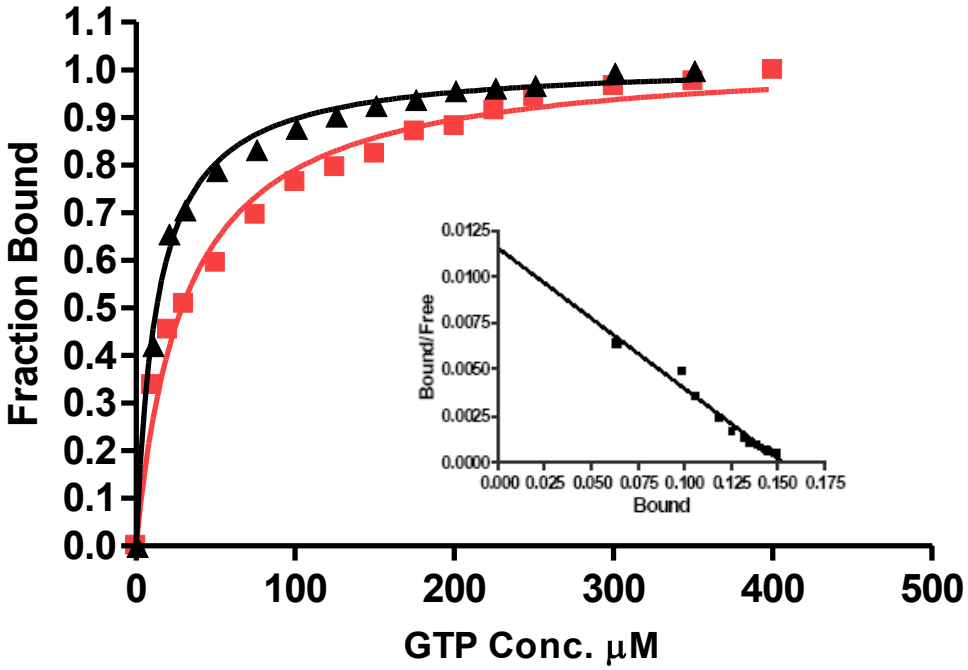

Figure 3. ***Fluorescence intensity measurements on binding of HCV NS5B Q65H mutant protein (▲) and wildtype(■) protein with GTP at 22°C. Inset: Scatchard plot of mutant protein.***

Complex	ΔH	ΔS	ΔG
NS5B Q65H +GTP	-55.2 kJ/mol	-95.5 J/mol	-27.1 kJ/mol
NS5B Wildtype +GTP	-41.8 kJ/mol	-53.6 J/mol	-25.6 kJ/mol

Table 2a. ***Thermodynamic parameters of HCV NS5B Q65H and GTP binding ΔH and ΔS values were determined from van't Hoff plot. However, ΔG values were calculated at 21°C using equation ΔG = -RT ln Keq.***

Complex	Kd at 10°C	Kd at 15°C	Kd at 21°C	Kd at 25°C
NS5B Q65H +GTP	5.7 ± 1.1 μ M	10.9 ± 1.3 μ M	15.4 ± 2.2 μ M	22.3 ± 2.4 μ M
NS5B wildtype +GTP	12.8 ± 1.0 μ M	16.0 ± 2.6 μ M	24.8 ± 2.5 μ M	

Table 2b. ***Equilibrium dissociation constants for the interaction of the HCV NS5B Q65H mutant and wildtype with GTP, at different temperatures.***

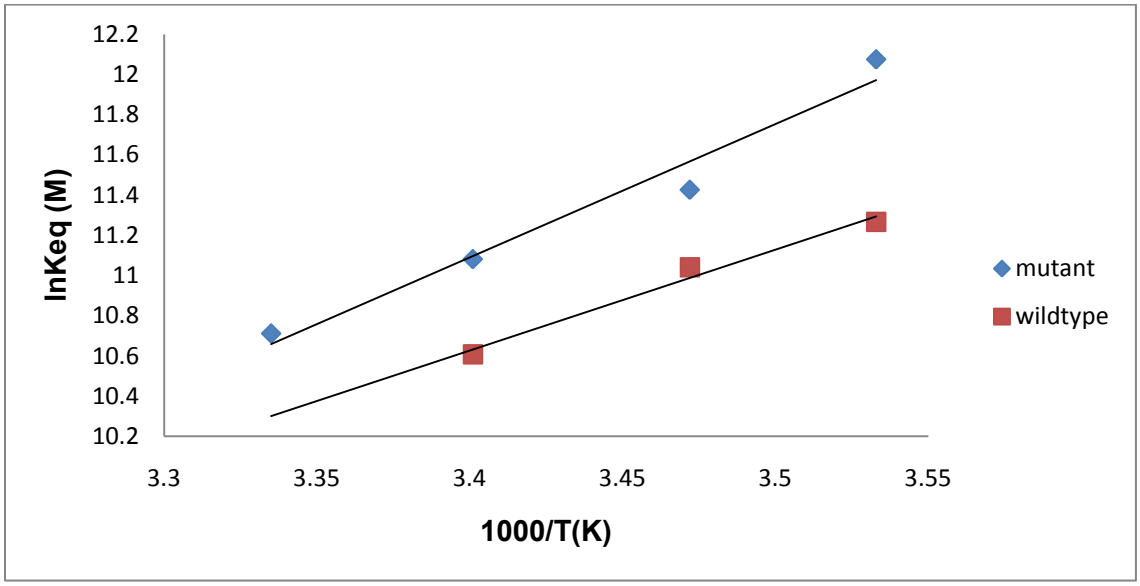

Figure 4. ***van't Hoff plot for the interaction of HCV NS5B Q65H(◊) and wildtype(■) protein with GTP.***

1.3.2. Fluorescence Titration of HCV NS5B Q65H mutant protein with GDP and $MgCl_2$

This is the first report to our knowledge of the interaction between this mutant structural protein and GDP. To determine the binding constants for the mutant structural protein with GDP, direct florescence studies were performed as shown in Figure 5. The K_d was calculated as described in Material and Methods. The binding of GDP with the mutant protein also resulted in a significant decrease in the emission fluorescence intensity.

The Q65H mutant exhibits a Kd of 11.7 ± 1.2 μM at room temperature. The inset in Figure 5 shows a of Scatchard plot. The straight-line generated by Graph Pad Prism 4.0 for bound/free versus bound ligand clearly demonstrates that there is one binding site for the GDP in the mutant protein. The K_d obtained by this program was similar to the one calculated by KaleidaGraph 4.0. The values for the dissociation constant were determined at different temperatures as shown in Table 3. From the temperature dependence of these dissociation constants, the thermodynamic parameters for mutant protein with respect to GDP were calculated (Table.4). A van't Hoff plot of ln Ka versus the reciprocal of temperature was used to calculate the thermodynamic parameters, entropy (ΔS), and enthalpy (ΔH). Figure 6 shows the van't Hoff plot based on GDP binding to Q65H mutant protein; the values of ΔS and ΔH were obtained from the intercept and slope, respectively (correlation coefficient>0.95).

As with GTP and GDP, we also studied the binding constants of $MgCl_2$ to mutant protein utilizing tryptophan fluorescence. The binding of the mutant protein with $MgCl_2$ resulted in the quenching of emission florescence intensities as observed earlier for the wild type protein [39]. The Kd of the NS5B Q65H protein when titrated with $MgCl_2$ was found to be 7.9 ± 2.0 mM. The reported value of K_d for the wildtype HCV structural protein was 3.1 mM [39]. Figure 7 shows Scatchard plot for $MgCl_2$ binding to mutant protein. The analysis revealed that there is one binding site for the $MgCl_2$ in the mutant protein as reported for wildtype protein [39]. Our results are reconfirmed by a similar K_d calculated by KaleidaGraph 4.0.

Complex	Kd at 10°C	Kd at 15°C	Kd at 21°C	Kd at 25°C
NS5B Q65H +GDP	10.2 ± 0.9μM	12.3 ± 1.2 μM	14.4 ± 1.1 μM	15.1 ± 1.5 μM

Table 3. ***Equilibrium dissociation constants for the interaction of HCV NS5B Q65H mutant with GDP.***

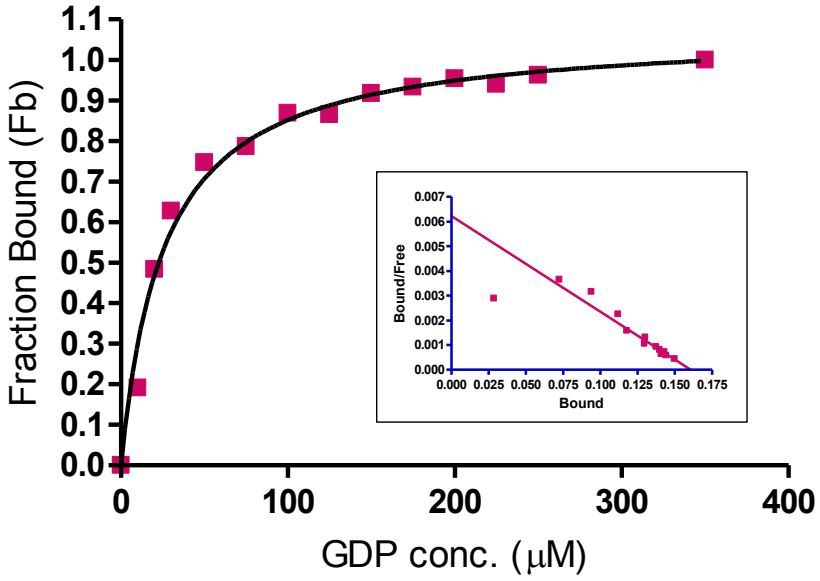

Figure 5. ***Fluorescence intensity measurements on binding of HCV NS5B Q65H mutant protein with GDP at 22 ºC.***

Complex	ΔH	ΔS	ΔG
NS5B Q65H +GDP	-16.6 kJ/mol	36.5 J/mol	-27.3 kJ/mol

Table 4. ***Thermodynamic parameters of HCV NS5B Q65H and GDP binding. ΔH and ΔS values were determined from van't Hoff plot. However, ΔG values were calculated at 21°C using equation ΔG = -RT ln Keq***

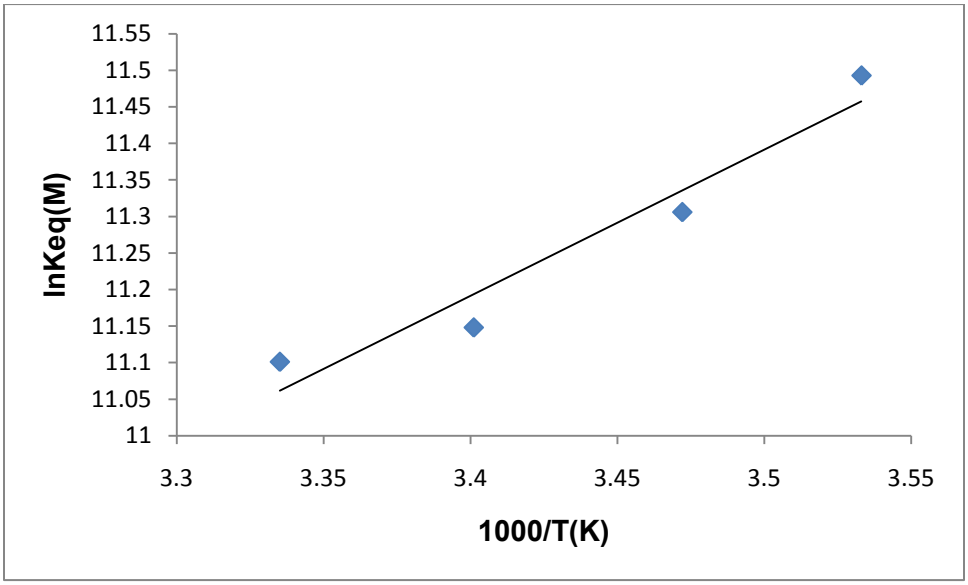

Figure 6. ***van't Hoff plot for the interaction of HCV NS5B Q65H(◊) with GDP***

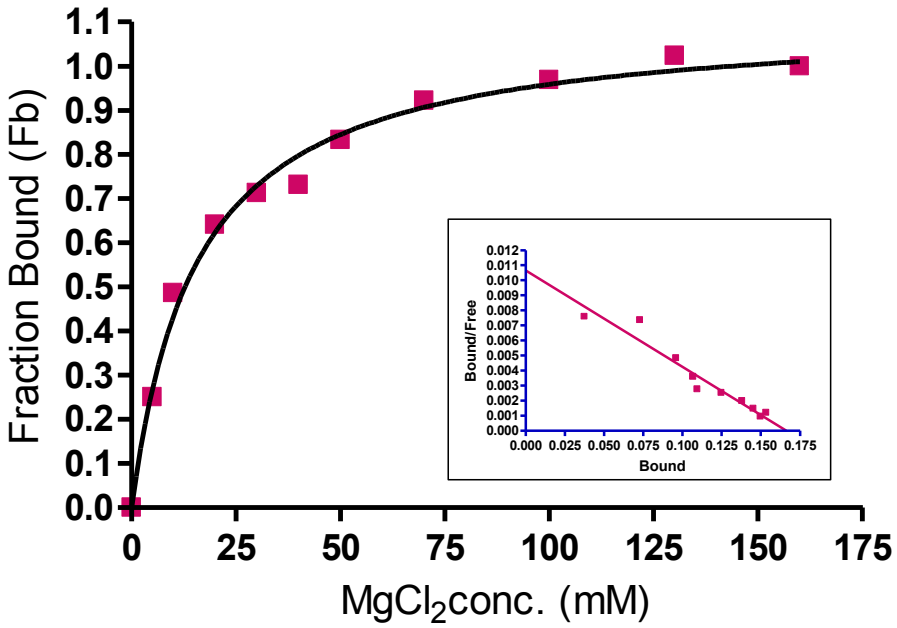

Figure 7. Fluorescence intensity measurements on binding of HCV NS5B Q65H mutant protein with $MgCl_2$.

1.3.3. Fluorescence Titration of HCV NS5B Q65H mutant protein with a 19mer RNA template alone and in the presence of GTP and $MgCl_2$

The binding of the HCV NS5B Q65H mutant protein to a single stranded RNA transcript LE19 [37] was also done in this study. This 19nt sequence is derivative of the 3' end of the minus-strand RNA of bovine viral diarrhea virus (BVDV). The three nucleotide unpaired initiation sequence in LE1 9 is predicted to form a simple stem-loop structure at the 3' end that directs initiation of *de-novo* RNA synthesis [37]. Similar to L19, but more stable structure is also found at the 3' end of the minus-strand HCV RNA [40, 41]. The titration of RNA template alone (Figure 8a) and in presence of GTP or $MgCl_2$ resulted in a decrease in emission fluorescence intensity upon RNA binding. The Q65H mutant exhibits a Kd of 9.7 ± 1.1 nM at 22°C. This was similar to what was earlier reported for the wild type protein i.e., 10 nM [39]. Figure 8b shows the saturation curve of the Q65H mutant protein with 19 mer RNA template alone and in presence of GTP or $MgCl_2$. Table 5 provides the Kd of three different combinations of mutant protein, GTP and $MgCl_2$ complexes with RNA template. Scatchard analysis was for the number of binding sites for RNA template in the mutant protein demonstrated that there was one binding site for the template in the mutant protein.

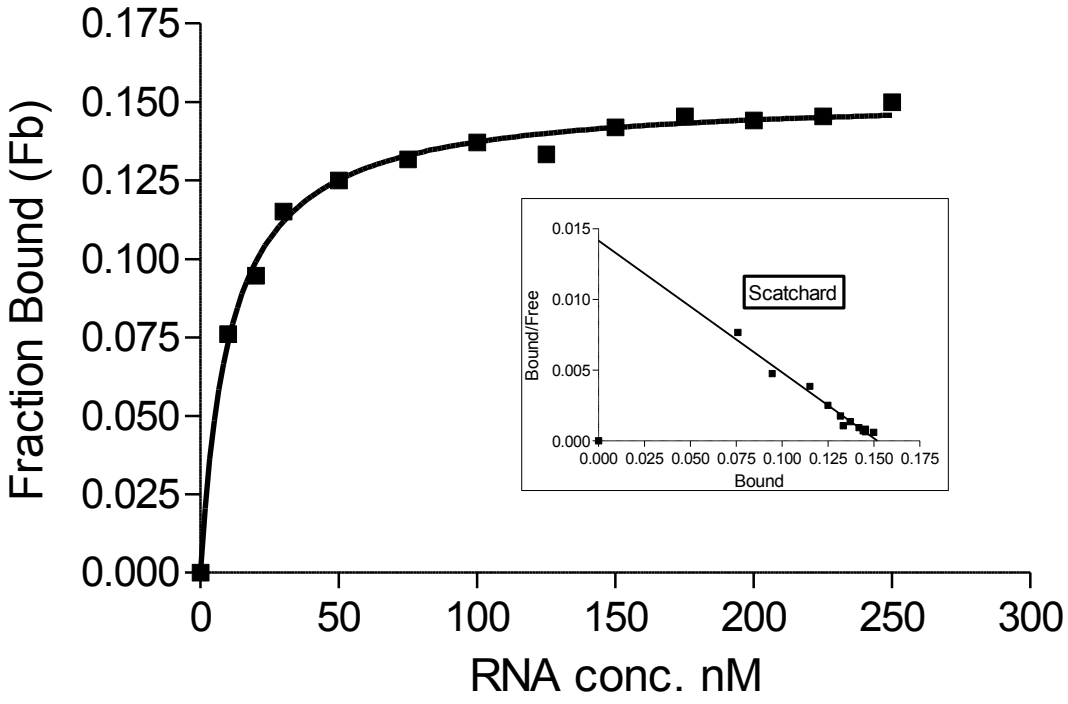

Figure 8(a). ***Fluorescence intensity measurements on binding of HCV NS5B Q65H mutant protein (■) with 19 mer RNA at 22°C. Inset: Scatchard plot of mutant protein.***

Complex	Kd
NS5B Q65H + RNA	9.7 ± 1.1 nM
NS5B Q65H + GTP + RNA	16.3 ± 3.5 nM
NS5B Q65H + $MgCl_2$ + RNA	13.7 ± 2.4 nM

Table 5. ***Equilibrium dissociation constants for the interaction of HCV NS5B Q65H mutant with 19 mer RNA template alone, and in presence of GTP or*** ***$MgCl_2$.***

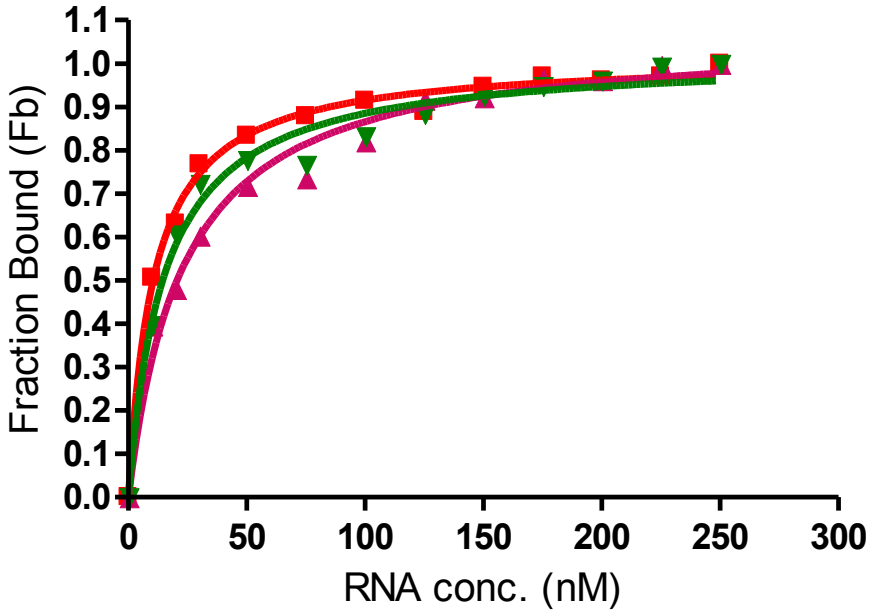

Figure 8b. ***Fluorescence intensity measurements on binding of HCV NS5B Q65H mutant protein with 19mer RNA template (■) alone, and in presence of GTP (▲) or $MgCl_2$ (▼) .***

1.4. Conclusions and Discussion

Hepatitis C virus is mainly responsible for non-A, non-B hepatitis [8, 42], leading to one of the most common chronic blood borne infections. This virus develops a high level of genetic diversity while circulating in infected individuals [43]. The main reason for this genetic diversity is the error prone replication by NS5B (non structural 5B), a key replicative enzyme present in this pathogen. NS5B adds the wrong nucleotides at the rate of 10^{-4} (approximately) generating a high degree of genetic variation in the circulating viruses in the patient [44, 45]. Further, there are reports that NS5B itself also accumulates multiple mutations over time. Some of these mutations that occur during infection may affect RNA dependent RNA polymerase (RdRp) activity [1].

In this study, we have characterized one mutant of NS5B with change of Gln to His residue at position 65 in the finger domain [1,10]. This Gln 65 His (Q65H) mutant is reported to have enhanced *in-vitro* RdRp activity by as much as 1.8 fold [1] and the reason for this increase in activity was not well understood in earlier studies.

The studies carried out by us revealed that mutant protein has a six-fold lower K_d for GTP than the wildtype protein, indicating that the mutant NS5B binds more tightly. The Q65H mutation comes into existence once the HCV infection has become chronic, suggesting there might be a link between this mutations in the

viral genome and the persistence of viral particles in the blood of the infected individuals.

This study also revealed the difference in the energetic and entropic characteristics of wild type and mutant protein during their interaction with GTP. The binding of GTP with both mutant and wildtype NS5B was found to be ethalpically favored and entropically unfavorable. The interaction of mutant NS5B with GTP had a more negative enthalpy as compared to the wildtype indicating a probable increase in electrostatic interactions. The entropy was less favorable indicating that the hydrophobic interactions are maybe less important. Further, the hydrophilic polar amino acid glutamine, located on the surface of the finger domain is replaced by the hydrophilic basic amino acid histidine that is a strong hydrogen and ionic bond former. This supports our results that the mutant protein has more negative enthalpy because of an increase in electrostatic interactions as compared to the wildtype protein. Probably, making the mutant protein structurally more favorable to carry on RNA dependent RNA polymerase reaction and resulting in a 1.8 fold increase in RdRp activity. The change in free energy was also found to be more negative for the mutant NS5B as compared to the wildtype protein, showing that binding of GTP to the mutant was more favorable and spontaneous. This putative change is probably providing some stability to this key protein and may relate to the viral persistence of this protein. This study shows Q65H differs in GTP binding from wildtype protein indicating binding of this ligand may be key to the enzymatic activity.

Chapter 2: Interaction of eIF4B with Zinc, Other Eukaryotic Translation Initiation Factors and Different Structural Elements of RNA

Eukaryotic translation/protein synthesis is a multistep process, involving translation initiation, elongation and termination steps. The entire cycle results in translation of mRNA into a nascent polypeptide chain. This is a crucial event in any living system for its survival. Numerous entities are involved in this process from translation initiation factors, mRNA, tRNA, ribosomes, various enzymes, and translation elongation factors to translation termination factors. Out of all this, translation initiation is a very important and regulatory step that decides whether a particular mRNA will undergo translation or not.

Eukaryotic translation initiation is an assembly process. The two subunits of the ribosome come together to the translation start site on the mRNA to begin synthesis of the polypeptide chain. This involves help from a large number of translation initiation factors and regulatory components. The next step in translation is elongation, during which the polypeptide continues to grow under the direction provided by template mRNA for the binding of a specific aminoacyl-tRNA to an elongating ribosome. The last step is translation termination, that is reached once the translation machinery along with ribosomes and mRNA reaches a stop codon, resulting in release of the nascent polypeptide to undergo further processing to form the final protein and all other components of the translation process go back to start a new cycle of protein synthesis.

2.1. Interaction eIF4B with Zn and other eukaryotic translation initiation factors

Eukaryotic translation initiation is a complicated process involving numerous translation initiation factors [46, 47]. The first step in this process is formation of a 43S pre-initiation complex consisting of a 40S ribosomal subunit along with Met-tRNAi and a few eukaryotic translation factors (eIF's). The next step is association of the 5'end of mRNA with the 43S pre-initiation complex and scanning of the mRNA for the start codon. Finally, the 60S ribosomal subunit associates with the complex to begin translation [48]. Several eIF's - eIF3, eIF4F (subunits eIF4G, eIF4E), eIF4B, poly A binding protein (PABP) etc., facilitate the interaction of 43S with the 5' end of mRNA. Of these, the interaction between three eukaryotic translation initiation factors (eIF's), namely eIF4F, eIF4A and eIF4B, is crucial for the proper occurrence of translation initiation [46]. EIF4A and/or eIF4F catalyze the hydrolysis of ATP to generate the energy that is essential for translation initiation [46, 49, 50]. The RNA-dependent ATP hydrolysis activity and ATP-dependent RNA helicase activity of eIF4A and eIF4F is enhanced by the presence of eukaryotic translation initiation factor 4B [2].

Eukaryotic translation initiation factor 4B is also reported to play an important role in organization and assembly of RNA and eIFiso4G, eIF4A, and poly(A)-binding protein(PABP)[2]. Cheng et. al. have recently identified eIF4B as a zinc binding protein [3]. We, along with our collaborator Prof. Gallie, reported that Zn

increases the RNA binding, homodimerisation, and interaction with PABP[3]. We have conducted biophysical studies on eIF4B using endogenous tryptophan fluorescence and fluorescently labeled RNA to understand the kinetics and binding of eIF4B with zinc and other eukaryotic translation initiation factors, especially with RNA during the translation initiation process. This study will help in a better understanding of basic translation initiation machinery and in revealing how Zn is involved in translation initiation and its regulation process.

2.1.1. Introduction

2.1.1.1. Eukaryotic Translation Initiation Factor 4B (eIF4B)

Wheat germ eukaryotic translation initiation factor 4B is a 59 kDa RNA-binding protein [46, 51]. The size of wheat eIF4B is 20 kDa smaller than mammalian eIF4B [46, 52]. Both wheat and mammalian eIF4B perform similar functions of enhancing the RNA dependent ATPase activity and ATP dependent RNA helicase activity of eIF4A and eIF4F during the translation initiation process [2, 53]. Eukaryotic eIF4B is also reported to interact with another translation initiation factor eIF3, which along with eIF4G is responsible for association of 43S pre-initiation complex to mRNA [54, 55]. It is likely that at this stage eIF4B facilitates the interaction of eIF3 with eIF4F to form the 48S complex [56] and thereby supports mRNA binding to the ribosome [2, 57-61]. Eukaryotic eIF4B also interacts with poly (A) binding protein (PABP) in both plants and animals [62-64]. The interaction of PAPB and eIF4B along with eIF4G increases the binding affinity of PABP for poly(A) RNA [63]. Wheat germ PABP is reported to increase the binding affinity of eIF4F and eIFiso4F to the 5’ cap on mRNA [65], and this binding is further enhanced by the presence of eIF4B along with PABP [66]. It has also been demonstrated *in vitro* that the interaction between PABP, eIF4G, and eIF4B, brings the two ends of mRNA in close proximity [67], a very important event to confirm whether the mRNA that is about to undergo translation is intact or not. If the poly(A) tail at 3’end is missing at this point, the mRNA will not be

able to bind PABP resulting in slow or abortive translation initiation and loss of binding of 40S translation initiation complex [2]. Thus, eIF4B performs multiple functions to facilitate the translation initiation process.

Three RNA binding domains are present in plant eIF4B. Mammalian and yeast eIF4B have only two RNA binding domains. Wheat eIF4B contains an extra novel N-terminal RNA binding domain, in addition to a conserved RNA recognition motif and a C-terminal RNA binding domain (Figure 9) [2]. The novel N-terminal domain in wheat is reported to interact with eIFiso4G through its C-proximal motif. This interaction is not known in eIF4B of any other species. Wheat eIF4B also has two binding sites for the PABP on either side of the C-terminal RNA binding domain. These binding sites contain conserved 41-amino acid repeats. Next to each repeat is a binding site for eIF4A. All these interactions by eIF4B suggests eIF4B performs multiple functions and helps the assembly and organisation process through interactions with several factors and RNA [2]. We have recently reported that wheat eIF4B is also a Zn binding protein [3].

The multiplicity of interactions makes eIF4B a very interesting target for study. Our study on eIF4B adds to the better understanding of eukaryotic translation initiation and regulation. In this study, we investigate the mechanism of the eIF4B and zinc interaction. Further, we also studied the binding of eIF4B with RNA and the preference for different RNA structures. This detailed study of eIF4B will further our understanding of how various viral RNAs use host translation

machinery for their own protein synthesis and will add another step towards understanding of the translation initiation and its regulatory process.

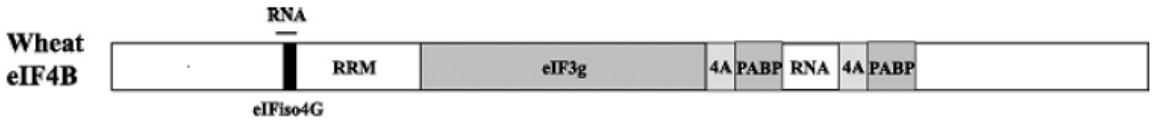

Figure 9. ***Domain organization of Eukaryotic Translation Initiation Factor 4B [2]***

2.1.1.2. Eukaryotic Translation Initiation Factor 4B (eIF4B) Mutants

Full length and different deletion constructs of wheat eIF4B were received from Prof. D. R. Gallie (Department of Biochemistry, University of California, California) in pGEX-2TK vector fused with GST tag. Each construct consists of different domain length of eIF4B, and differs in binding characteristics with respect to RNA, eIF4A, PABP and other translation initiation factors (Figure 3). GST-eIF4B- (1-527) is a full length eIF4B construct. GST-eIF4B- (69-527) lacks the novel N-terminal RNA binding domain. GST-eIF4B- (320-527) contains the C-terminal RNA binding domain. GST-eIF4B- (340-527) is our control without any RNA binding domain. GST-eIF4B- (69-360) contains shortest region of the second RNA binding domain [2].

Figure 10. ***Eukaryotic translation initiation factor 4B deletion constructs, showing the number of trptophan residues and different binding properties with respect to 4A, PABP, RNA and eIFiso4G[2]***

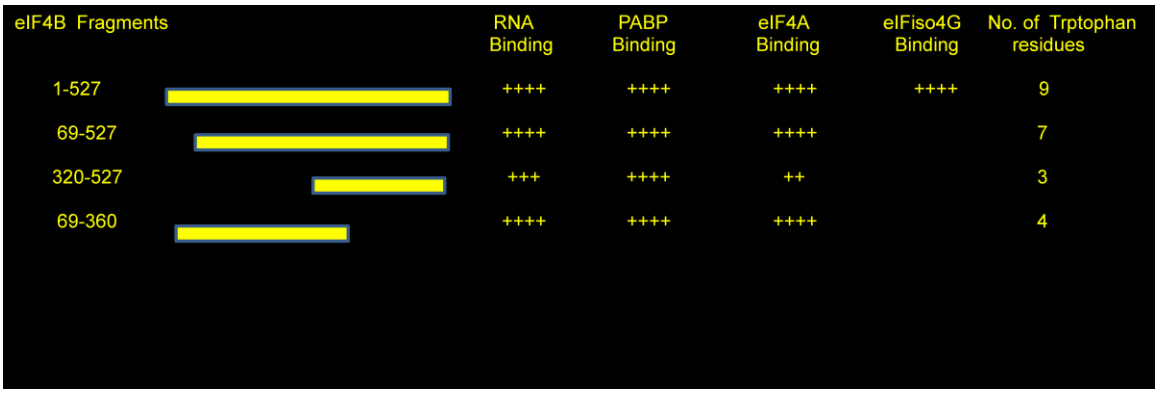

2.1.1.3. Fluorescence Spectroscopy

Fluorescence spectroscopy is discussed in section 1.1.2 of this thesis.

2.1.1.4. Circular Dichroism

Circular dichroism (CD) is a very useful technique to study the secondary structures in proteins. CD utilizes the difference in absorption of left handed polarized light and right handed polarized light when it passes through the optically active molecule. Circular dichroism measures the secondary structure in the wavelength range 190-250 nm (far-UV region). This wavelength corresponds to the absorption by peptide bond and the analysis of CD spectrum of this regions reveals the information about secondary structures such as helices and beta sheets [68]. Each native protein has a characteristic CD spectrum. Any change in structure due to its environment, interaction with ligands or other moieties results in the variation of characteristic CD spectra for that protein. This analysis is used to understand the interactions and changes in secondary structure occurring due to various biological events. The positive and negative maxima, the shape of the spectral curve etc. give specific details of perturbations occurring within the protein structure [69]. For example, the alpha helical structures are described by 'w'-shaped spectra with troughs around 222 and 208 nm in the far-UV region while the beta sheet structures are defined by a 'v'-shaped spectra with a trough around 217–220 nm [69].

Ellipticity is the main unit for circular dichroism. When the components of differentially absorbed left handed polarized light and right handed polarized light are put together, they result in elliptically polarized light. This ellipticity is defined as the tangent of the ratio of the minor to major elliptical axis [69]. Other units of CD are molar ellipticity (and mean residual ellipticity (MRE). We have used circular dichroism to understand the effect of increasing concentration of zinc on the secondary structures of eukaryotic translation initiation factor 4B.

2.1.1.5. *In-vitro* Translation and Luciferase Assay

In-vitro translation is a very useful method of translating any mRNA into its polypeptide product in a cell free system. This technique is useful to study translation of a particular mRNA without any effect of transcription, post-translational processing, and protein trafficking etc. [70]. Wheat germ lysate is one of the commonly used *in-vitro* translation systems with the advantage of low cost and low endogenous mRNA levels [71]. This provides minimal background during the *in-vitro* translation study. Wheat germ lysate efficiently translates exogenous mRNA from a wide variety of sources in a cell free system [72]. The *in-vitro* translation system also helps to understand the effect of various factors on the rate of translation of particular mRNA.

Once the translation of mRNA is complete, the level of translated polypeptide is determined using different assays and techniques. The luciferase assay is a popular method to measure the rate of translation. The *luc*-gene coding for luciferase enzyme is added to the designed transcript, which is translated along with the desired mRNA. The product of *luc*-gene is an oxidative enzyme luciferase that oxidizes lucifernin in presence of ATP to a luminescent product that can be measured [73]. The amount of luminescence produced is directly proportional to the amount of *in-vitro* translation of *luc*-gene. Thus, this is a very useful tool to study the rate of translation of a particular mRNA. We have used wheat germ *in-vitro* translation system to study the effect of zinc on translation of control mRNA containing the *luc*-gene. The level of *in-vitro* translation was then analyzed using a luciferase assay.

2.1.2. Material and Methods

2.1.2.1. Expression and Purification of Wheat EIF4B and its Mutants

We received the full length and domain deletion constructs containing our eIF4B inserts of interest fused with GST tag in pGEX-2TK vector, from our collaborator Prof. D. R. Gallie, Department of Biochemistry, University of California, Riverside, California. The first step was to scale up the amount of plasmid received. Transformation was done by heat shock method using DH5α cells. The transformed cells were then selected on LB agar plate containing 100 µg/ml ampicillin. After selection, a single colony was picked and inoculated in 10 ml LB media containing 100 µg/ml ampicillin for plasmid isolation. The plasmid isolation protocol is described in the appendix. For protein expression the BL21 (DE3) pLys S cells are transformed with the isolated plasmids. The transformed cells were then selected on an LB agar plate containing 100 µg/ml ampicillin.

Cells containing pGEX-2TK vector containing eIF4B inserts of interest fused with GST tag were selected by colony selection and inoculated into 15 ml LB media with 100 µg/ml Ampicillin. After being grown overnight, the culture was transferred to I.2 liter LB medium with 100 µg/ml Ampicillin. After being grown to an absorbance of 0.6 OD_{600}, the cells were treated with 0.1 gm/L isopropyl β-D-thiogalactopyranoside (IPTG) in order to induce protein expression and further incubated for overnight. Cells containing the vector were selected by colony

selection. The pellets were collected by centrifugation for 15 min and 7000 rpm at 4°C and resuspended in 1X cold PBS (50 µl/1 ml culture, or 50 ml for 1 L) containing one Roche-complete protease inhibitor cocktail tablet. Cells were lysed by sonication by short bursts until disrupted. Cells were spun at 12,000 g for 10 min at 4°C to pellet down cell debris. The supernatant was collected and subjected to ultra-centrifugation at 40,000g for 2 hrs. The supernatant was collected and passed through 45 µm filter before loading into 1 ml GSTrap FF column. The protein was eluted using elution buffer (50 mM Tris HCl, 10 mM reduced glutathione pH 8.0). The protein containing fractions were immediately pooled. The dialysis was performed using 1XPBS buffer to remove glutathione from the protein preparation. The concentration of purified protein was calculated using a Bradford assay. The purified protein was then stored at -80°C for further studies.

2.1.2.2. Expression and Purification PABP

Glycerol stock of BL21 (DE3) pLys *E. coli* containing pET19b construct with a PABP insert was plated on LB agar plate containing 100 µg/ml ampicillin and 34 µg/ml chloramphenicol. The cells containing pET19b vector containing the PABP insert of interest fused with a His tag were selected by colony selection and inoculated into 15ml LB media with 100 µg/ml ampicillin. After being grown overnight, the culture was transferred to I.2 liter LB medium with 100 µg/ml

ampicillin and 34 µg/ml chloramphenicol. After being grown to an absorbance of 0.6 OD_{600}, the cells were induced with 0.1 gm/L isopropyl β-D-thiogalactopyranoside (IPTG) and further incubated overnight. Cells containing vectors were also selected by colony selection. The pellets were collected by centrifugation for 15min and 6000 rpm at 4°C and resuspended in binding buffer (5 mM Imidazole, 0.5 M NaCl, 20 mM Tris HCl pH 7.9) containing one Roche-complete protease inhibitor cocktail tablet. Cells were lysed by sonication by short bursts until disrupted. Cells were spun at 15,000 g for 15 min at 4°C to pellet down cell debris. Supernatant was collected and ultra centrifuged at 40,000 g for 2 hrs. The supernatant was collected and passed through a 45 µm filter before loading into Novagen His•Bind® column containing Ni^{2+}-charged His•Bind Resin. The protein was collected in 20 mM Tris-HCl (pH 7.9), 500 mM NaCl, and 1 M imidazole using His-bind kit protocol (Novagen). The protein containing fractions were immediately pooled. Dialysis was performed using 20 mM Tris-HCl (pH 7.6), 0.15 mM NaCl to remove imidazole from the protein preparation. The samples were passed through a 0.22 µm filter (Millipore) before conducting the spectroscopy measurements. The concentration of purified protein was calculated using a Bradford assay. The purified protein was then stored at -80°C for further studies.

2.1.2.3. Fluorescence Measurements

Fluorescence measurements were carried out at 22 °C on a SPEX Fluorolog-τ-2 spectrofluorometer equipped with a high-intensity (450 W) xenon arc lamp. Excitation and emission slit widths of 2.0 mm and 3.0 mm were used, and a path length of 1.0 cm was employed. All chemicals were molecular biology grade. Binding experiments were performed using 50 nM and 150 nM eIF4B (1-527) protein to which increasing amounts of $ZnCl_2$, $MgCl_2$ and poly (A) RNA were added individually in different experiments. To study the competition between Zn^{2+} and Mg^{2+} metal ion for the binding sites in the protein, eIF4B (1-527) was titrated with $MgCl_2$ in the presence of 1000 nM $ZnCl_2$. The background emission was eliminated by subtracting the signal from buffer containing an appropriate quantity of substrate. Data were averages of three or more titrations. All experiments were performed using an excitation wavelength of 280 nm to monitor the emission at 332 nm. The binding buffer used for all fluorescence studies consisted of 20 mM HEPES, 100 mM KCl (pH 7.6).

2.1.2.4. Data Treatment

The fluorescence was normalized by using the formula $f_b = (F_0 - F_{obs})/(F_{obs} - F_\infty)(F_0/F_\infty) + (F_0 - F_{obs})$, which is directly related to the fraction of protein bound (f_b), where F_{obs} is the observed fluorescence, F_0 is the fluorescence observed in

the absence of any metal ion (that is the fluorescence of the protein) and F_{∞} is the fluorescence at saturation. The normalized fluorescence was used to determine the equilibrium dissociation constant (K_d). The details of the data fitting are described elsewhere [46, 65, 74] Nonlinear least squares fitting of the data were performed using KaleidaGraph software Version 4.

2.1.2.5. Circular dichroism

Far UV-Circular dichroism spectra for the full length eukaryotic translation initiation factor 4B were collected on a CD Spectrometer Model 202-01 from Aviv Biomedical Inc. The spectra were measured in 10 mM sodium phosphate, 100 mM NaCl pH 7.4 buffer. Measurements were done in a 1.0 mm path length quartz cuvette at 22ºC. Each spectrum is the average of 10 scans. The 200 µg/ml protein concentration was used for all measurements. After each addition of zinc, the sample was incubated for at least 15 minutes before taking the reading.

2.1.2.6. Wheat Germ Lysate Preparation

Natural raw wheat germ (Bob's Red Mill, Oregon) was used for the preparation of wheat germ lysate for luciferase activity. Lysate was prepared according to a

published procedure [75]. Wheat germ was converted to fine powder by vigorously mixing with alumina powder and grinding in a pre-chilled mortar and pistil. Powdered wheat germ was mixed well with buffer E (20mM HEPES.KOH, pH 7.6, 1mM $Mg(OAc)_2$, 2 mM $CaCl_2$, 6 mM β-mercaptoethanol, 120 mM KCl, 0.1 mg/ml of soybean trypsin inhibitor and 0.5 mM PMSF. The mixture was then centrifuged at 15000 g for 20 min at 4°C. Fatty acids as top layer were discarded and the remaining supernatant was passed through a Sephadex G-25 column. Fractions were collected starting with the emergence of material that absorbed at 260 nm and ending when absorbance dropped below 90 units/ml. Absorbance for the pooled fraction was measured and aliquots of prepared wheat germ lysate were stored at -80°C.

2.1.2.7. *In-vitro* Translation and Luciferase Assay

In-vitro translation was carried out in wheat germ lysate supplemented with 10 µM complete amino acid mixture (Promega), 50 units of RNase inhibitor, luciferase assay buffer (25 mM Tricine, pH 8.0, 5 mM $MgCl_2$, 0.1 mM EDTA supplemented with 33.3 mM DTT (dithiothreitol), 0.25 mM coenzyme A, and 0.5 mM ATP) for luciferase activity, 1µg of luciferase control RNA (Promega) with and without 200 µM zinc chloride. The translation reactions were incubated at 22°C for 2 hrs. Luciferase activity was calculated by measuring light emitted upon

addition of 0.5 mM luciferin. Each reaction was conducted in duplicate/triplicate and constant volume was maintained for all reactions.

Results

2.1.3.1. Interaction of Full-Length eIF4B and Zn

This is the first biophysical study characterizing the interaction of eukaryotic translation initiation factor 4B and zinc. We reported, along with our collaborator Prof. Gallie that wheat protein eIF4B is a zinc binding protein [3]. The binding was found to affect some characteristic eIF4B properties such as homodimerization, binding with RNA, and interaction with poly(A)-binding protein [3]. These findings prompted further investigation into the mechanism of binding of eIF4B with zinc in order to determine any regulatory role of this interaction on the overall eukaryotic translation initiation process.

The intrinsic florescence of eIF4B on zinc binding was used in the present studies to calculate the K_d (Figure 11). The wheat eIF4B exhibits a K_d of 19.7 ± 1.6 nM at 22°C [3]. This low K_d clearly indicates that there is a very tight interaction between eIF4B and zinc.

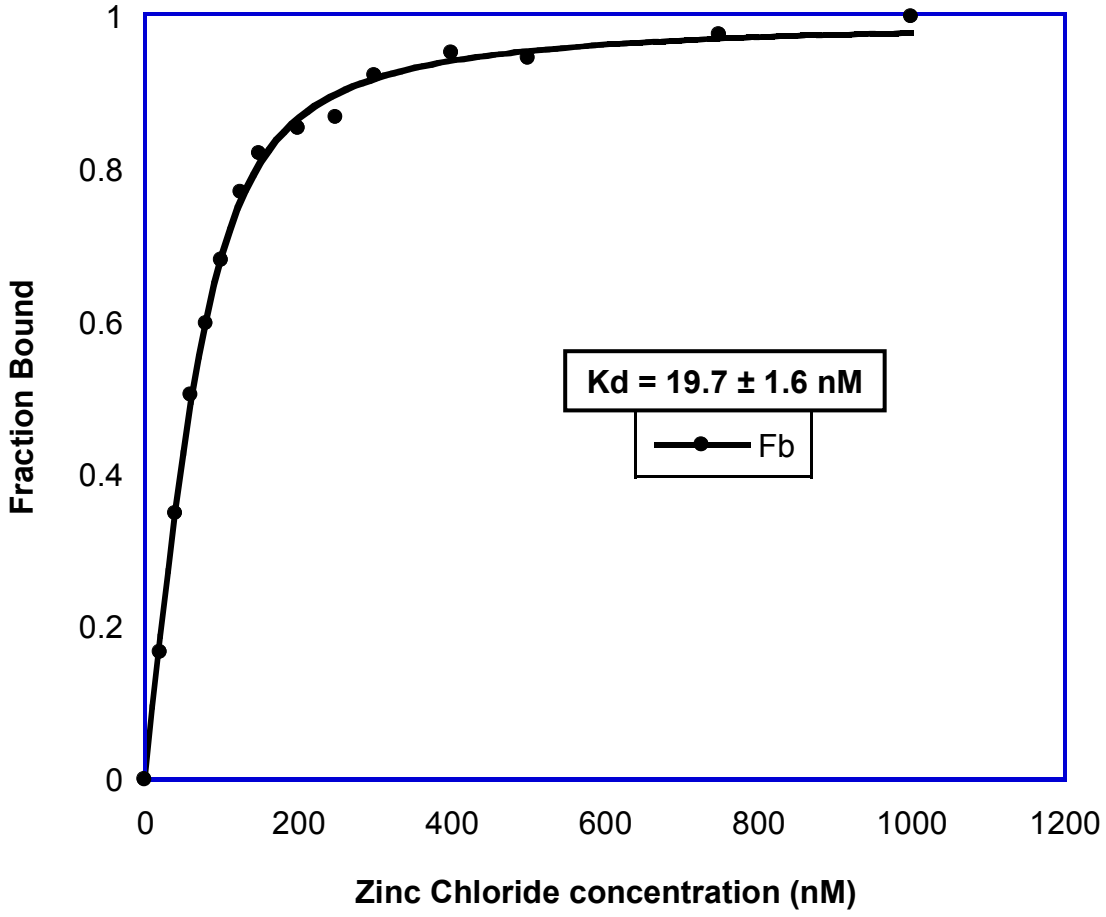

Figure 11. ***Fluorescence intensity measurements on binding of full length eIF4B with zinc chloride at 22°C [3].***

2.1.3.2. Interaction of EIF4B Deletion Mutants and Zn

Next, we wanted to see if the binding of zinc and its effect is associated with any particular domain. To study this, we used various deletion constructs of eIF4B containing different domains. Each construct consists of a different domain length of eIF4B, and differs in binding characteristics with respect to RNA, eIF4A, PABP and other translation initiation factors. GST-eIF4B- (1-527) is a full length eIF4B construct. GST-eIF4B- (69-527) lacks the novel N-terminal RNA binding domain. GST-eIF4B- (320-527) contains the C-terminal RNA binding domain. GST-eIF4B- (69-360) contains second RNA binding domain [2].

To determine the binding constants for the deletion mutant protein with zinc, direct florescence studies were performed as shown in Figures 12, 13 and 14. The K_d was calculated as described in Material and Methods.

The binding data revealed that zinc interacts most tightly with full length eIF4B. However, as the deletion extends towards the C-terminal, zinc binding decreases. This study was not successful in localizing the zinc binding to a specific domain.

Complex	*Kd (nM)*
eF4B(1-527) + $ZnCl_2$	**19.7 ± 1.6**
4B(69-360) + $ZnCl_2$	**45.1 ± 5.0**
4B(69-527) + $ZnCl_2$	**59.8 ± 7.6**
4B(320-527) + $ZnCl_2$	**79.7 ± 4.5**

Table 6. ***Equilibrium dissociation constants for the interaction of full length eIF4B and its deletion mutants with zinc chloride determined by fluorescence titration at 22°C.***

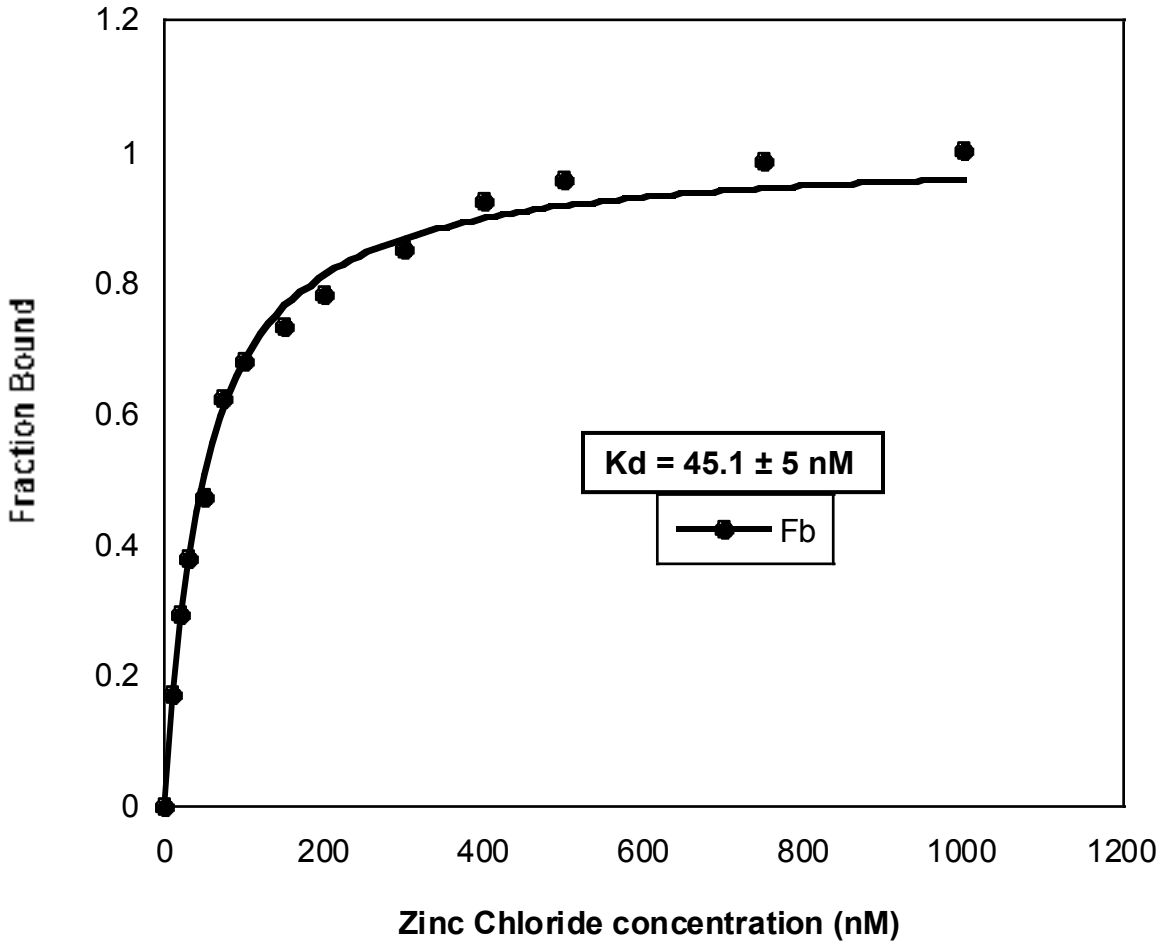

Figure 12. ***Fluorescence intensity measurements on binding of eIF4B(69-360) with zinc chloride at 22°C.***

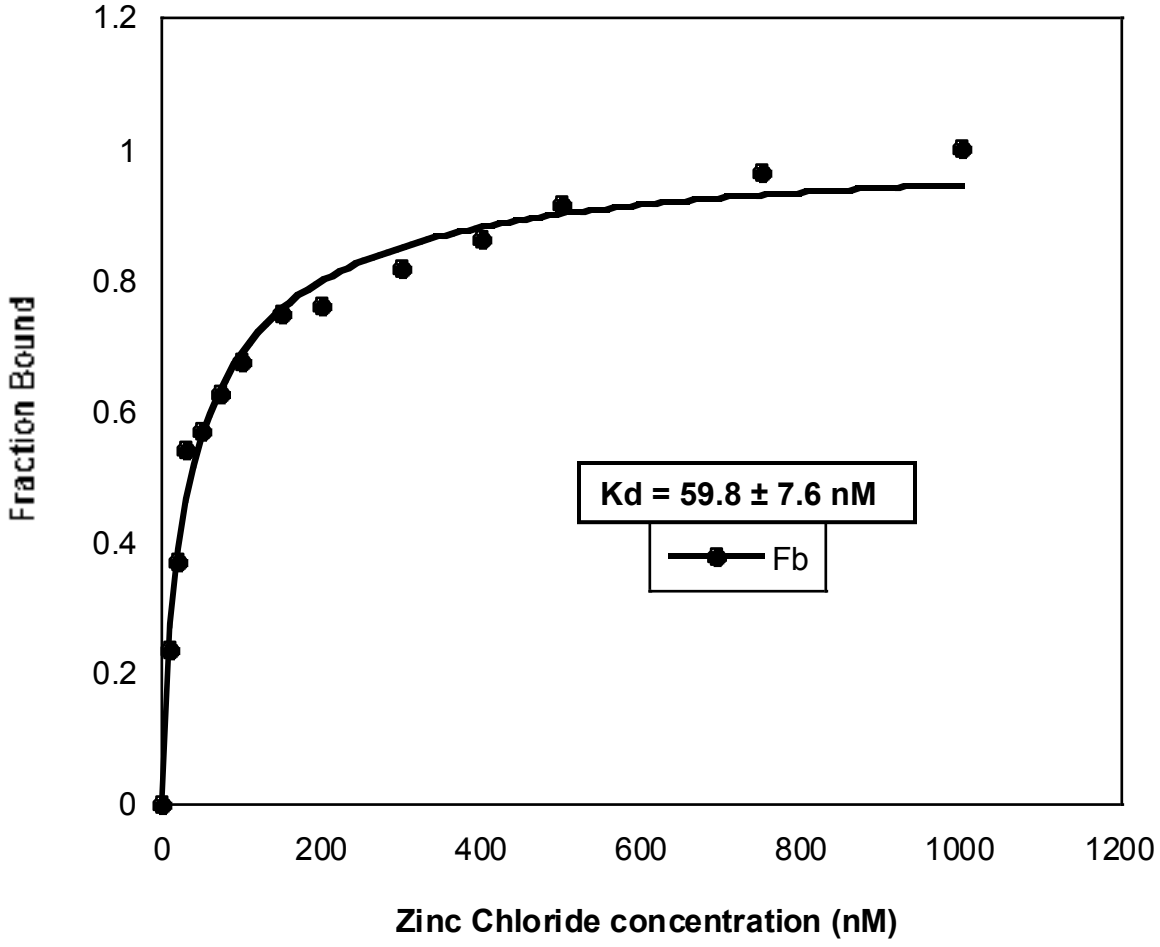

Figure 13. ***Fluorescence intensity measurements on binding of eIF4B(69-527) with zinc chloride at 22°C.***

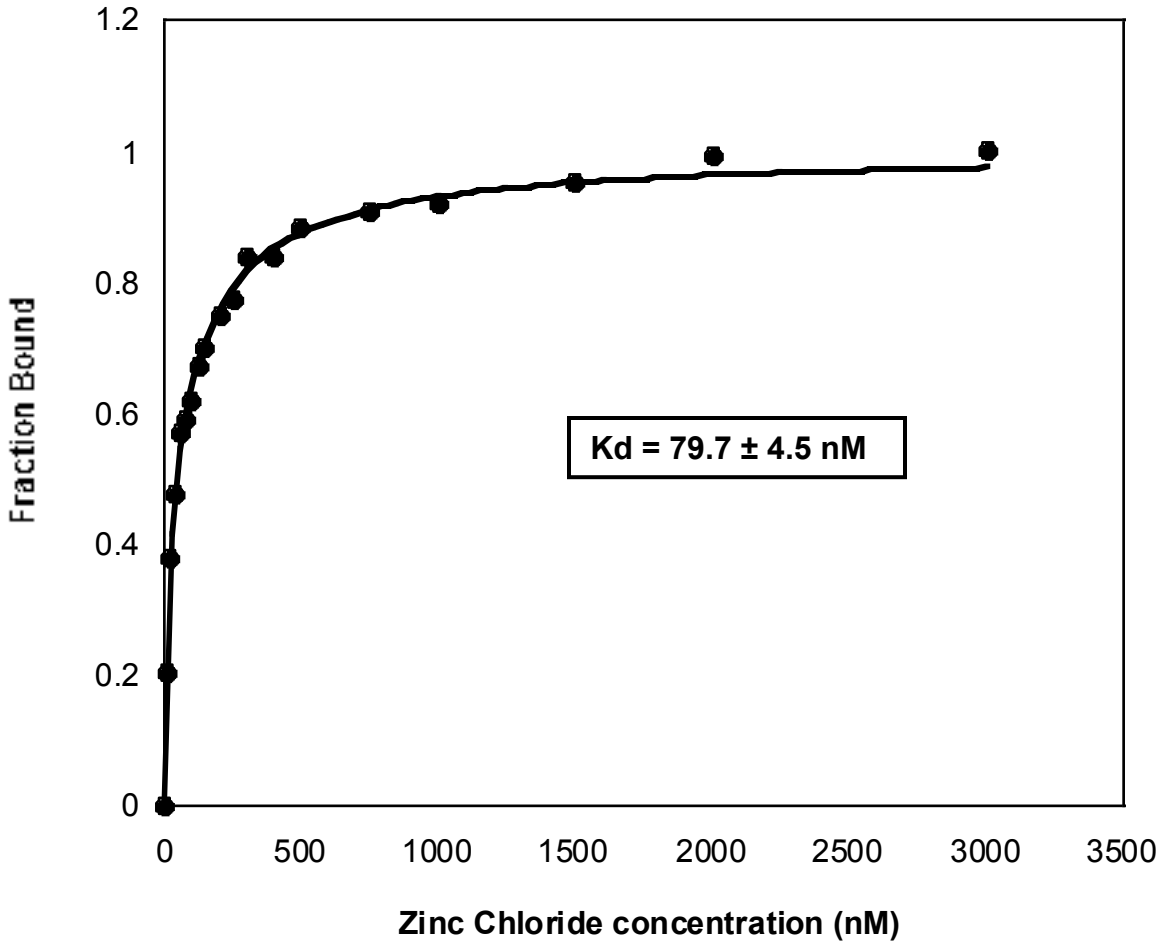

Figure 14. ***Fluorescence intensity measurements on binding of eIF4B(320-527) with zinc chloride at 22°C.***

2.1.3.3. Interaction of EIF4B and other Divalent Metal Mg with/without Zn

Magnesium bound eIF4B with a K_d of 42.4 ± 5.3 nM, showing that eIF4B binds zinc more strongly than it does magnesium [3]. The K_d for Mg^{2+} was virtually unchanged when 1000 nM Zn^{2+} was included in the analysis (Table 7), suggesting that Mg^{2+} binds to eIF4B independently of Zn^{2+} [3]. It is noted that monovalent ion potassium was also present in titration buffer to stabilize the protein. The effect of other monovalent ions on eIF4B was not studied.

PABP and zinc binding affinities were also studied to observe if the interaction with zinc is specific to eIF4B or not. Results showed a much weaker interaction with PABP (K_d = 33.6 ± 5.8 μM) than eIF4B. The Kd was calculated by fitting the titration curves by KaleidaGraph 4.0 as discussed in Material and Methods.

Complex	*Kd*
eF4B(1-527) + $ZnCl_2$	**19.7 ± 1.6nM**
eIF4B(1-527) + $MgCl_2$	**42.4 ± 5.3 nM**
eIF4B(1-527).$ZnCl_2$ + $MgCl_2$	**40.1 ± 5.1 nM**

Table 7. ***Equilibrium dissociation constants for the interaction of full length eIF4B with zinc chloride and magnesium chloride (in presence and absence of 1000nM zinc chloride).***

2.1.3.4. Interaction of EIF4B full length/eIF4B mutant and Poly (A) RNA with/without Zinc

After studying the interaction of zinc with eIF4B and its mutants and the effect of divalent ions, we further investigated the effect of zinc on other properties such as RNA binding of eIF4B. The binding studies of eIF4B full length and (320-527) deletion mutant with poly (A) RNA with/without zinc was carried out. The 320-527 mutant contains only the C-terminal RNA binding domain. The binding of poly (A) RNA with the eIF4B full length and mutant protein resulted in a decrease in the emission fluorescence intensities.

Data analysis revealed that full length eIF4B and the 320-527 deletion mutant show similar binding with RNA (Table.8). The binding of proteins to RNA became tighter with proteins upon addition of zinc. The full length eIF4B protein exhibits a K_d of 77 ± 7 nM at room temperature, while the (320-527) mutant protein exhibited a K_d of 61.9 ± 6.4 nM. The value of the dissociation constant for both proteins was significantly decreased upon addition of zinc, giving a K_d of approximately 45 ± 3 nM.

Similarity in the values of K_d and the changes on addition of zinc, indicates that probably the RNA binding and the observed effect on addition of zinc is mainly from the C-terminal domain of the eIF4B protein.

	20mer poly (A) RNA (nM)
4B(1-527)	77.0 ± 7
4B(320-527)	61.9 ± 6.4
4B(1-527) +20 μM ZnCl2	45 ± 3

Table 8. ***Equilibrium dissociation constants for the interaction of eIF4Bfull length/ mutant with poly A RNA alone, and in the presence of 20 μM of*** $ZnCl_2$.

2.1.3.5. Circular dichroism analysis of interaction of eIF4B and Zn

To better understand how the binding of zinc affects eIF4B structure circular dichroism analysis was conducted. Circular dichroism is a useful tool to study secondary structures and we used it to study the effect of zinc on the secondary structure of full length eukaryotic translation initiation factor 4B. The addition of zinc to eIF4B resulted in a change in CD spectra (Figure 15).

The circular dichroism analysis revealed that addition of zinc to eIF4B results in a change in alpha helical content of eIF4B. eIF4B contains approximately 12% alpha helix in its secondary structure. The addition of increasing amount of zinc resulted in more than 50% decrease in alpha helical content of the protein. After addition of 200 μM of zinc, no further significant change was observed in circular dichroism spectra of eIF4B (Figure 16).

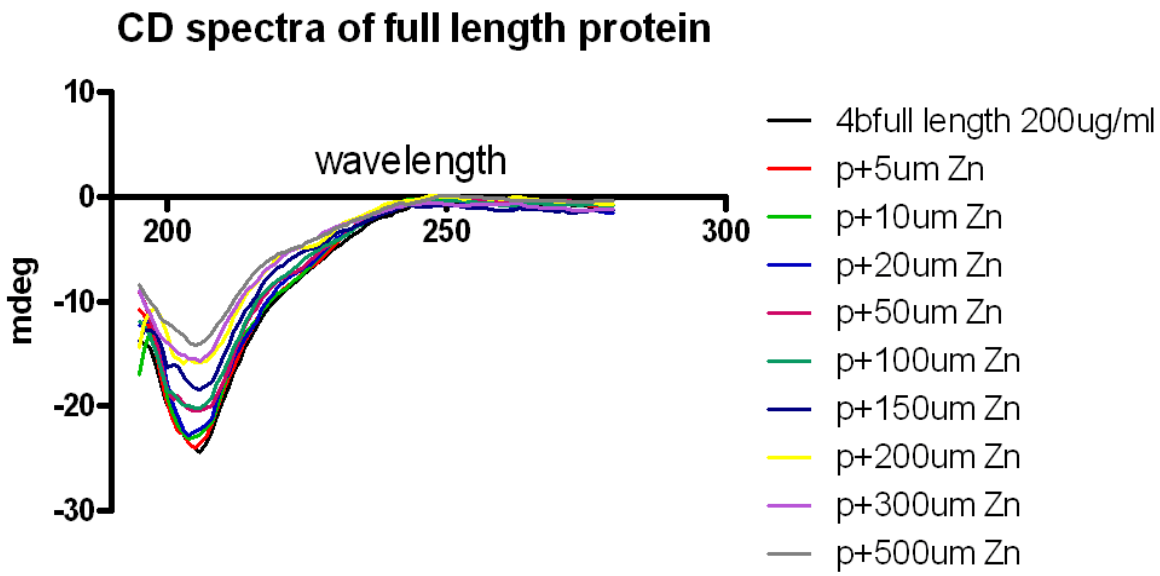

Figure 15. ***CD analysis of full length eIF4B alone and in the presence of different concentrations of $ZnCl_2$.***

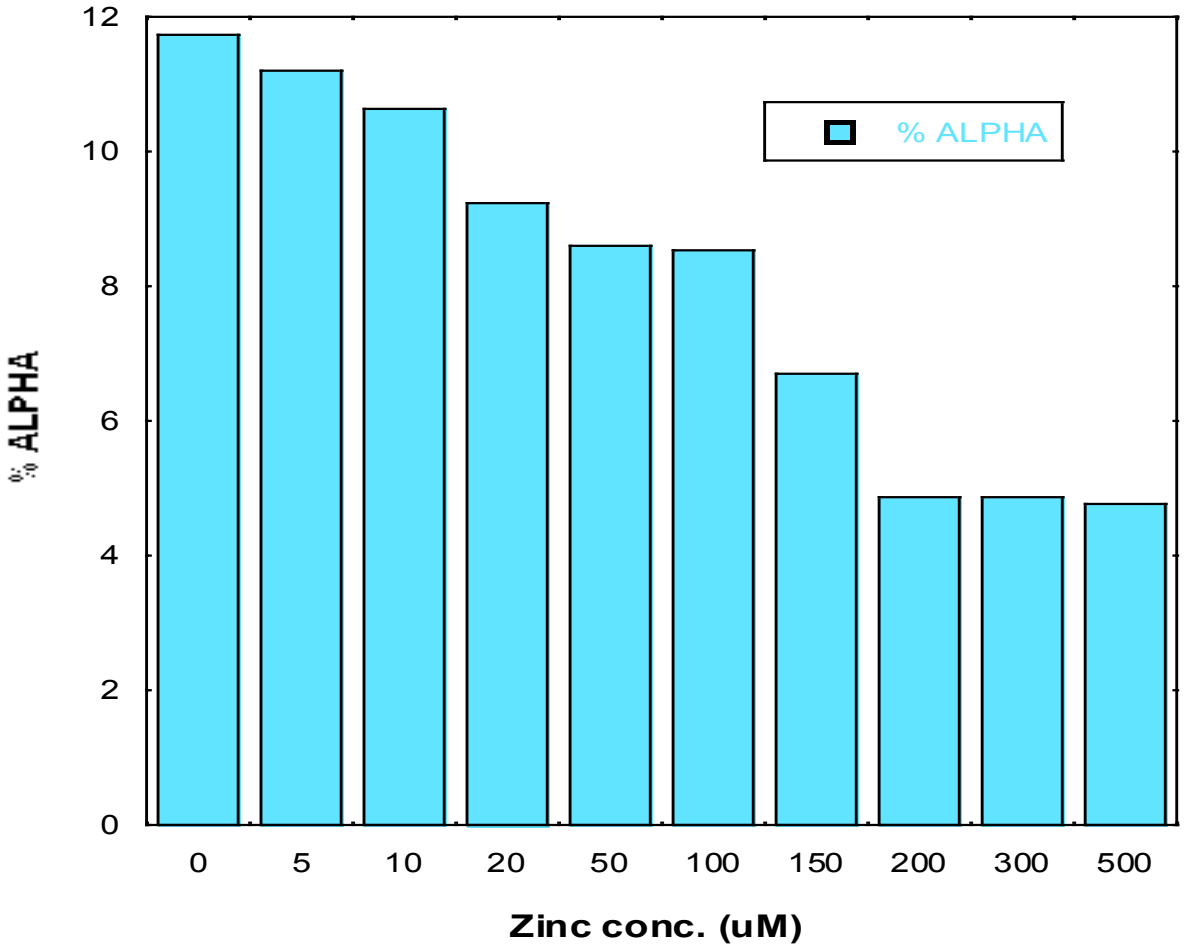

Figure 16. ***Change in Alpha content of full length eukaryotic translation initiation factor 4B with increase in Zn concentration.***

2.1.3.6. Effect of Zn on *In-vitro* Translation of Wheat Germ Lysate and Luciferase Assay

The structural analysis from fluorescence studies and circular dichroism of eukaryotic translation factor eIF4B and zinc showed that zinc binds very tightly with eIF4B. Interaction of zinc with eIF4B resulted in a change in secondary structure of eIF4B. The next step in this study was to do analysis of the effect of zinc on eIF4B in a biological system.

The wheat germ lysate was prepared in the laboratory as described in Material and Methods. Control RNA containing *luc*-gene (Promega) was used for translation. *In-vitro* translation of control RNA was conducted in wheat germ lysate in the presence and absence of zinc. This reaction was followed by a luciferase assay to measure the emission of light as a result of oxidation of luciferin by luciferase enzyme (product of *luc*-gene) using a luminometer.

Our results indicate that addition of zinc enhances the rate of in-vitro translation in wheat germ lysate. This is a biological assay supporting our biophysical analysis of effect of zinc on eukaryotic translation initiation factor 4B. The increase in the rate of translation in in-vitro system on addition of zinc suggests that it plays some regulatory role in the eukaryotic translation initiation process.

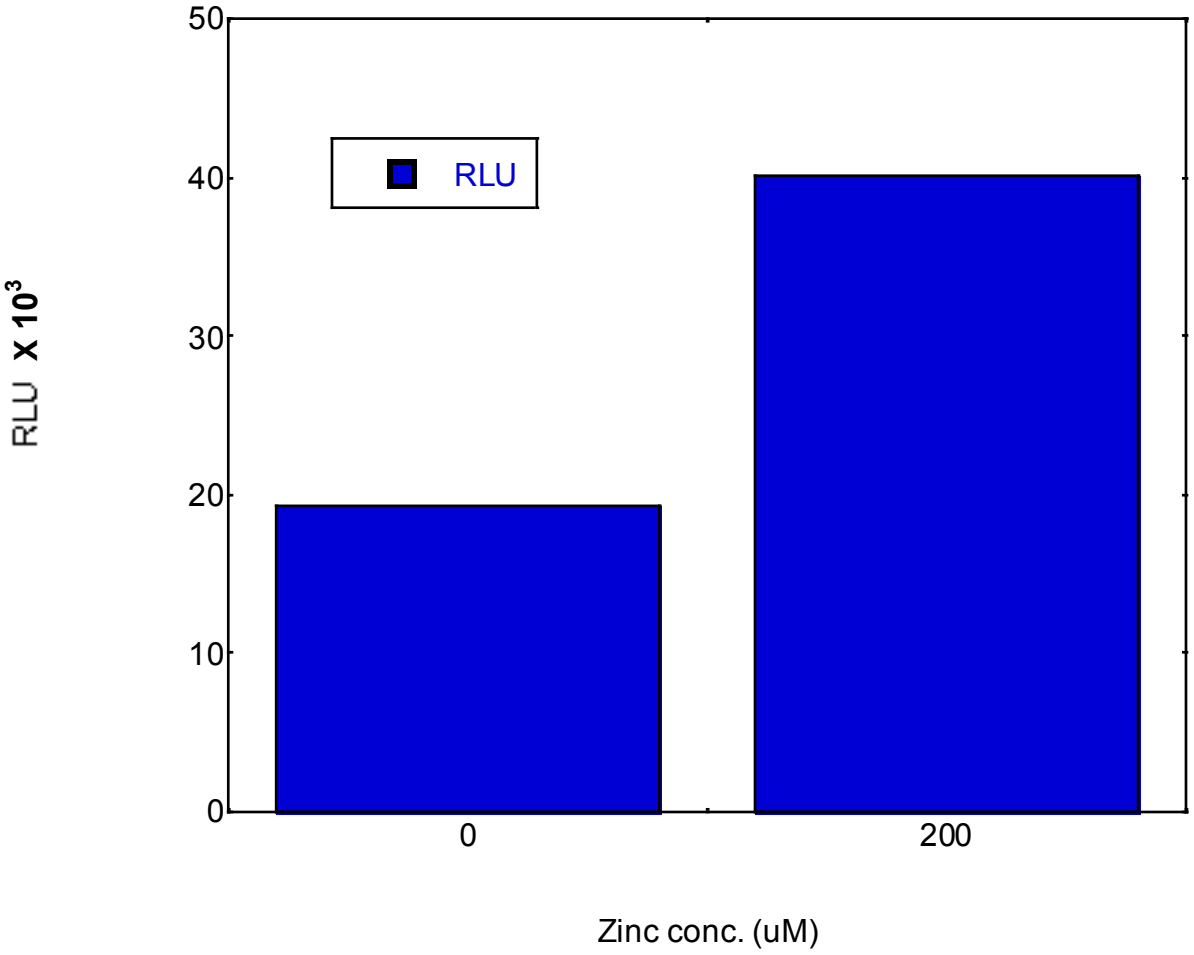

Figure 17. ***The effect of zinc on in-vitro translation of control luciferase RNA in wheat germ extract. First bar showing in-vitro translation without zinc and second bar showing in-vitro translation in presence of 200 µM zinc.***

2.1.3.7. EIF4B, PABP and 29 mer RNA interaction

To study the effect of zinc on eIF4B and other translation initiation factors, equilibrium dissociation constants for their binding were studied. We studied the binding of eukaryotic translation initiation factor 4B and poly (A) binding protein (PABP). The K_d was calculated as described in Material and Methods. EIF4B and PABP bind very tightly with each other, K_d of 11.1 ± 1.1 nM similar to the value reported earlier [62]. The 29 mer RNA oligo with fluorescein tag at 3'end (described in Material and Methods) was designed to study the binding of eIF4B with any RNA molecule in the presence of PABP and later also with zinc. We labeled the oligo because we wanted to study its interaction with the protein complex. It is difficult to perform complex binding analysis using intrinsic protein fluorescence because of the involvement of two proteins in the experiment. The RNA molecule contained a small 5 nucleotide loop and 4 base stem with unpaired bases on either side of this structure. The eIF4B showed a very tight binding both in thepresence and absence of PABP with this structure. The extent of tight binding between these factors and RNA was at the limit of concentration measurements, and the data with picomolar concentrations are not possible. This imposed a limit for us to further investigate the effect of zinc on these interactions.

The binding between eIF4B and 29mer stem loop RNA as compared to poly (A) was more than 40 fold tighter. This interesting result raised the question of

whether eIF4B binds differently with different RNA structures. We investigated this further, and the findings of this study are elaborated in chapter 2.2 of this study.

COMPLEX	Kd (nM)
eIF4B + RNA	1.8 ± 0.6 (Less than 2nM)
eIF4B + PABP	11.1 ± 1.1
eIF4B.PABP + RNA	1.6 ± 0.5 (Less than 2nM)

Table 9. ***Equilibrium dissociation constants for the interaction of 29mer RNA with eIF4B alone, and eIF4B full length complexed with PABP, as determined by fluorescence anisotropy.***

2.1.4. Conclusions and Discussion

Eukaryotic translation initiation factor 4B is an important part of translation initiation process. We found in our biophysical study that wheat eIF4B binds very tightly with zinc with a K_d in the low nM range. Upon binding with zinc, the fluorescence spectra of the protein showed a significant decrease in the emission fluorescence intensities, indicating that upon binding with zinc the conformation of eIF4B is changed.

Next, we were interested in finding if the zinc binding property is specifically associated with any particular domain of eIF4B. We used different domain deletion constructs of eIF4B that differ in binding characteristics with respect to RNA, eIF4A, PABP and other translation initiation factors. The binding data revealed that zinc interacts most tightly with full length eIF4B. This study was not successful in precisely defining the zinc binding domain.

Further, we investigated if this effect is specific to zinc or can be demonstrated by any divalent ion. We observed that the binding of eIF4B with magnesium ion, is weaker compared to zinc and the K_d for magnesium was virtually unchanged when 1000 nm zinc was included in the analysis, suggesting that magnesium binds to eIF4B independently of zinc. In the biochemical studies, our collaborator also found similar results and observed that the presence of other divalent ions,

Mg^{2+}, Ca^{2+}, or Mn^{2+} had no effect on eIF4B self-association [3]. This outcome clearly indicates that the binding of eIF4B is specific to zinc.

The above results lead to the question, if this binding is so specific then what is the effect of zinc on other properties of eIF4B? To answer this, the RNA binding property of eIF4B was studied. The effect of zinc on the interaction of eIF4B and poly (A) RNA was investigated. The results indicated that the presence of zinc results in tighter interaction of eIF4B and poly(A) RNA. The C-terminal domain was found to have a greater effect with RNA binding in the presence of zinc as reported earlier in the biochemical study [3]. This C-terminal RNA binding domain actually plays a crucial role in the assembly process. The binding site for eIF4A and two binding sites for the poly(A)-binding protein are present in a region within each of two conserved 41-amino acid repeat domains on either side of the C-terminal RNA binding domain, supporting a central role for this conserved eIF4B domain in facilitating interaction with other components of the translational machinery [2]. This makes it structurally a better target for the binding with the RNA template.

The CD analysis showed that the presence of zinc results in significant change in the secondary structure of protein. The alpha helix was reduced more than 50% at 200 μM zinc concentration. We have also conducted a secondary structure prediction using predict protein server [76]. The server analysis revealed that there is approximately 11.4% helix in the full length protein. Further details

showed that out of 11.4% helix more that 90% of it is located in C-terminal part of the protein. Our collaborator along with our earlier results suggested that the sequence C-terminal to the C-terminal RNA binding domain is probably required to have the complete stimulatory effect of zinc on eIF4B [3]. The computational analysis also pointed to this region where the maximum percentage of alpha helix is present. The CD data revealed that this helical secondary structure is changed on addition of zinc. This result is supported by the CD investigation conducted by another member of the lab on eIF4B 69-527 mutant. She observed that 69-527 mutant showed more than 60% reduction in alpha helix on addition of 200 μM zinc. The percentage alpha helix content of the overall protein increased in the mutant lacking the N-terminal domain and the change in alpha helix also increased. This is definitely due to the presence of most of the alpha helical content in the C-terminal region of the protein.

Interestingly, zinc belongs to a group of metals that has a preference for the imidazole ring of histidine residues in proteins [77, 78]. eIF4B has seven histidine residues that could potentially interact with zinc. Sequence analysis revealed that out of seven His residues, six are present in the C-terminal region of the protein starting after residue number 320. Interaction with His residues may explain why the effect of zinc is most prominent on the C-terminal region of eIF4B.

The computational analysis, fluorimetric result and CD data together were able to address the question “how does zinc affect the functions of eIF4B”? Upon

binding with eIF4B zinc causes a change in secondary structure of eIF4B, (mainly helical structure in the C-terminal domain of the protein) that makes the protein conformation more favorable for dimerization, RNA binding, and interaction with other eukaryotic translation initiation factors. The C-terminal domain of eIF4B is very critical in this sense as it has most of the other interacting protein binding sites and it becomes more favorable structurally in the presence of zinc.

eIF4B can serve, as an important therapeutic target, since its role in the binding of the scaffold protein eIF4G, is regulatory during the assembly of the initiation complex. The assembly of various entities at initiation, the complexity and organization of eukaryotic translations initiation factors, the presence of RNA and the recruitment of the ribosomal complex resulting in synthesis of a native polypeptide is a complex process that is not well understood. It is the aim of these studies to elucidate the role of the eIF4B and eIF4B-Zn at this highly complex site. This study is particularly important in plants since zinc is one of the key nutrients in their system. Further studies will determine if the amount of zinc in soil, and the amount absorbed by plants also determines the level of translation initiation in plants. This will improve our understanding of growth and development of various systems and the effects of the environment upon it.

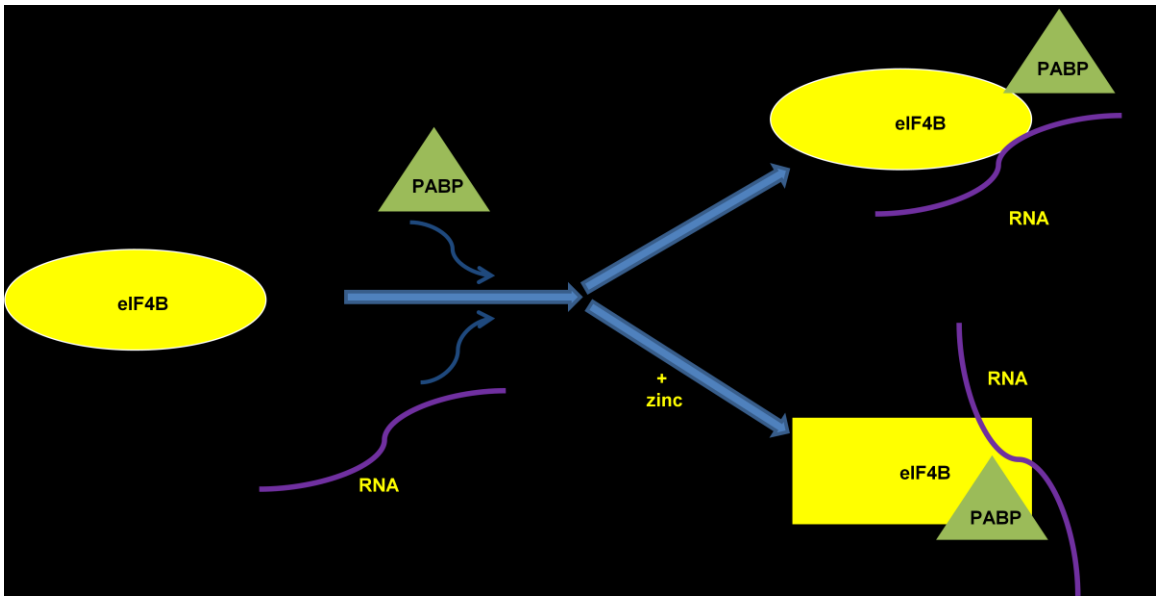

Figure 18. ***Schematic representation of interaction of eIF4B with the RNA and PABP during eukaryotic translation initiation process in the presence and absence of zinc. (i) In absence of zinc the interaction is weak and without any change in conformation of eIF4B. (ii) In the presence of zinc the change in conformation of eIF4B take place and the interaction is strong.***

2.2. Interaction of eIF4B with Different Structural Elements of RNA

2.2.1. Introduction

2.2.1.1. eIF4B and RNA structure

Eukaryotic translation initiation factor 4B is an RNA binding protein whose function is to enhance the RNA-dependent ATPase activity and ATP-dependent RNA helicase activity of eIF4A and eIF4F during the translation initiation process [2, 53]. Eukaryotic eIF4B also interacts with another translation initiation factor eIF3, which along with eIF4G is responsible for association of the 43S pre-initiation complex to mRNA [54, 55]. Probably at this stage, eIF4B facilitates the interaction of eIF3 with eIF4F, to form the 48S complex[56] and supports mRNA binding to the ribosome [2, 57-61].

Earlier studies suggested that translation of mRNA with moderately stable secondary structure in the 5' leader is highly stimulated in yeast by eIF4B as compared to the mRNA with little secondary structure [2, 79]. It was observed that during the selection process the RNA recognition motif (RRM) of eIF4B showed more preference for binding to RNA with a stem loop structure [2, 80]. Further, in the presence of eIF4A, the C-terminal domain is the primary domain responsible for RNA affinity but in its absence, RRM also plays a significant role [2, 80]. However, there is a lack of binding data and equilibrium constants.

During the studies of the effect of zinc on binding of eukaryotic translation initiation factor 4B, we observed the binding of eIF4B with structured RNA was found to be 40 times tighter than poly A RNA. It was already known that eIF4B is a RNA binding protein and this result suggested that eIF4B may be involved in the selection of RNA during the translation initiation process.

To better understand the role of eIF4B in the selection of RNA, we studied the interaction of eIF4B with structurally different RNAs and the effect of eIF4A on this interaction.

2.2.1.2. EIF4A

Eukaryotic translation initiation factor 4A is an RNA helicase, an RNA- dependent ATPase and ATP-dependent RNA binding protein [81-85]. EIF4A is prototypical of a large family of helicases known as the DEAD-box family [86]. The DEAD-box name is given because of the presence of a conserved sequence of four D-E-A-D amino acid residues.

EIF4A, eIF4B and eIF4F together are crucial for binding of the ribosome with mRNA. The primary role of eIF4A in cap-dependent translation initiation is to

unwind the secondary structure present in the 5' UTR of mRNA to facilitate the ribosome binding and scanning for the initiation codon.

Binding and hydrolysis of ATP and its hydrolysis by eIF4A leads to a change in the conformation of the protein and its affinity for RNA. There are a number of structural studies of eIF4A in open and closed conformations. It was reported that eIF4A has only a very weak helicase activity on its own [87] and cannot process because it dissociates from ssRNA faster than it hydrolyses ATP [81, 82, 85, 88]. EIF4B promotes the RNA-dependent ATPase activity and ATP-dependent RNA helicase activity of eIF4A.

EIF4A is present in both the free form and as a part/subunit of eIF4F in eukaryotes, binding to two sites in mammalian eIF4G and to a single site in yeast eIF4G [82, 89-91].

2.2.1.3. Fluorescence Anisotropy

Fluorescence anisotropy is a very useful biophysical tool to study the interaction between two proteins or protein and their ligands and helps to determine the binding constant between them. The theory behind this phenomenon is if we pass a polarized light through a fluorophore it will also further emit the polarized light. The amount of polarized light emitted depends on the location, size and

movement of the fluorophore. Upon interaction with the larger molecule, the fluorophore tumbling gets reduced. This results in an increase in polarized signal which can be used to determine various biophysical parameters. For our experiments, a fluorophore was present on the smaller of the two entities so that the effect of binding could be clearly observed.

The method to calculate the anisotropy is shown in Figure 18. Firstly the sample is excited with linearly polarized light and the polarizer is used to measure the emission intensity. The polarizer can be oriented either parallel or perpendicular to the plane of polarization of the incident beam. Depending on its orientation the observed light intensities are called $I_{\parallel}$ (I parallel) or $I_{\perp}$(I perpendicular). These intensities are then used to calculate anisotropy (r) [4].

$$r = \frac{I_{\parallel} - I_{\perp}}{I_{\parallel} + 2I_{\perp}}$$

The change in the anisotropy of various small 29mer RNAs, labeled with fluorecein upon binding with eIF4B or eIF4B and eIF4A complex is used to calculate the binding constants in this study. The anisotropy data was fitted to the following equation to determine the dissociation equilibrium constant [92, 93]

$$r_{obs} = r_{min} + \{(r_{max} - r_{min})/(2\times[^{Fl}RNA])\}\{b - (b^2 - 4[^{Fl}RNA][eIFs])\text{^}0.5\}$$

where, $b = K_d + [^{FI}RNA] + [eIFs]$, r_{obs} is the observed anisotropy for any point in the titration curve, r_{min} is the minimum observed anisotropy in the absence of protein, r_{max} is the maximum anisotropy at saturation and is fit as a parameter. Nonlinear least squares fitting of the titration data was performed using KaleidaGraph software 4.

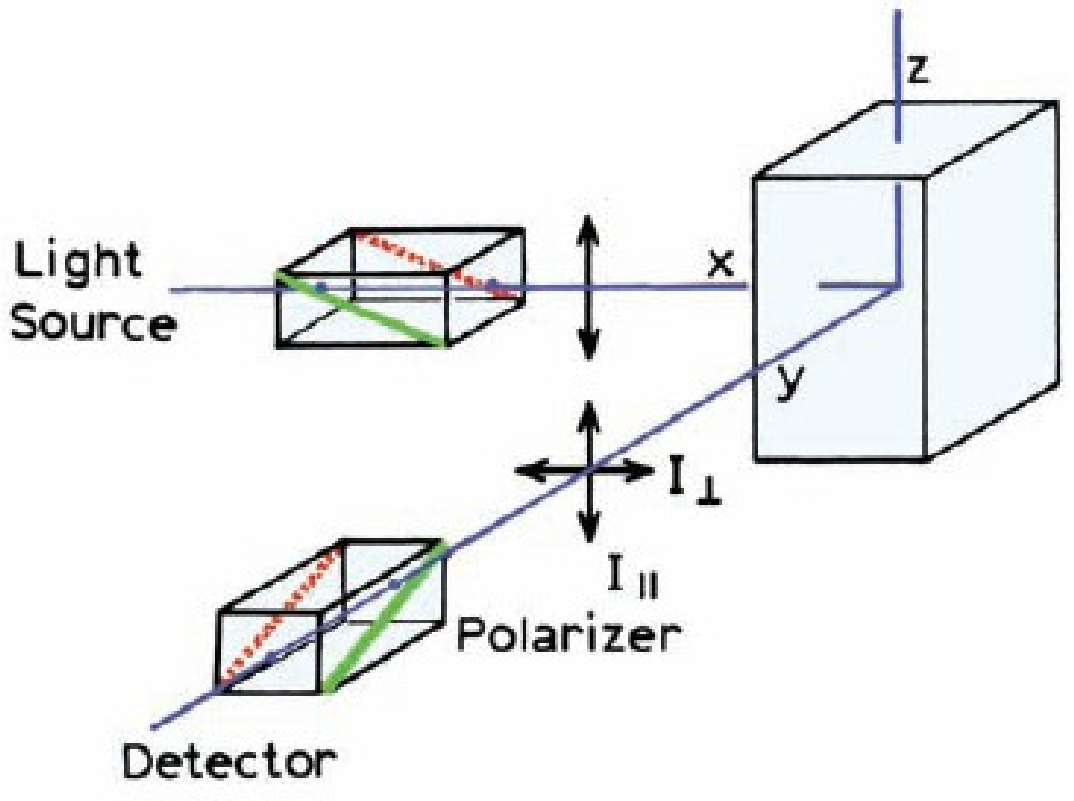

Figure 19. Schematic representation *of Florescence Anisotropy [4]*

2.2.2. Material and Methods

2.2.2.1. Materials

Five 29 mer RNA were designed with different secondary structures using RNAfold [94-96] software. All RNA and 20mer poly A RNA were purchased from Genelink Hawthorne, NY. All RNA except 20mer poly A RNA and partially double stranded RNA has a fluorecein label at the 3' end.

29 mer RNA sequences used in the study (structures are shown in Table 10):

1) 29mer RNA.

5' GGGAAGGAAGGUCGAAAGGACCAACAGCU 3'

2) 29mer linear RNA (29merlinear).

5' GGGAAGCAACGAGGAAGGGAUCAACAGUU 3'

3) 29mer RNA with 8 nucleotide loop(29mer8loop) .

5' GGGAUCGGAUGAAGCACCGGGUAAACAGC 3'

4). 29mer RNA with 5 nucleotide loop and base paired stem (29mer5loopcomplete bp).

5' GGGUAAGGAAGGCUGAACCUUCCUUACCC 3'

5) Partial double stranded RNA oligo. (Fluorescein label at 5' end of smaller strand).

a). 14mer RNA(14merRNAfluor) with fluorescein label at 5' end (smaller strand)

5' GGGGCAGCGCAGCG 3'

b). 35mer RNA (35merRNA) (larger strand)

5' GGGACCAUGGAACAACAUUAUCGCUGCGCUGCCCC 3'

2.2.2.2. Expression and Purification of eIF4B

A plasmid containing full length eIF4B was received from Prof. D. R. Gallie, Department of Biochemistry, University of California, Riverside, California). The first step was to scale up the amount of plasmid received. Transformation was done by heat shock method using DH5α cells. The transformed cells were then selected on LB agar plate containing 100 µg/ml ampicillin. After selection, a single colony was picked and inoculated in 10 ml LB media containing 100 µg/ml ampicillin for plasmid isolation. The plasmid isolation protocol is described in the Appendix. For protein expression the BL21 (DE3) pLys S cells were transformed with the isolated plasmids. The transformed cells were then selected on LB agar plate containing 100 µg/ml ampicillin.

Cells containing pGEX-2TK vector containing our eIF4B inserts of interest fused with GST tag were selected by colony selection and inoculated into 15ml LB media with 100 µg/ml ampicillin. After being grown overnight, the culture was transferred to I.2 liter LB medium with 100µg/ml ampicillin and grown to 0.6 $OD_{600.}$ The cells were induced with 0.1gm/L isopropyl β-D-thiogalactopyranoside (IPTG) and further incubated for overnight. The pellets were collected by centrifugation for 15 min, 7000 rpm at 4°C and resuspended in 1X cold PBS (50 µl/1 ml culture, or 50 ml for 1 L) containing one Roche-complete protease inhibitor cocktail tablet. Cells were lysed by sonication by short bursts until disrupted. Cells were spun at 12,000 g for 10 min at 4°C to pellet down cell debris. Supernatant was collected and ultra centrifuged at 40,000 g for 2 hrs. The supernatant was collected and passed through a 45 µm filter before loading into 1ml GSTrap FF column. The protein was eluted from the column using elution buffer (50 mM Tris HCl, 10 mM reduced glutathione pH 8.0). The protein containing fractions were immediately pooled and dialysed using 1XPBS buffer to remove glutathione from the protein preparation. The concentration of purified protein was calculated using a Bradford assay with BSA as standard. The purified protein in 1X PBS was then stored at -80°C for further studies.

2.2.2.3. Expression and Purification of eIF4A

For protein expression the BL21 (DE3) pLys S cells are transformed with the isolated plasmids containing eIF4A insert. The transformed cells were then selected on LB agar plate containing 100 µg/ml ampicillin and 34 µg/ml chloramphenicol. Cells containing pET23d vector containing our eIF4A inserts of interest fused with his tag were selected by colony selection and inoculated into 15 ml LB media with 100 µg/ml ampicillin and 34 µg/ml chloramphenicol. After being grown overnight, the culture was transferred to I.2 liter LB medium with 100 µg/ml ampicillin and 34 µg/ml chloramphenicol. After being grown to 0.6 OD_{600} and induced with 0.1 gm/L isopropyl β-D-thiogalactopyranoside (IPTG) and further incubated for overnight. The pellets were collected by centrifugation for 15 min and 6000 rpm at 4°C and resuspended in binding buffer (5 mM Imidazole, 0.5 M NaCl, 20 mM Tris HCl pH 7.9) containing one Roche-complete protease inhibitor cocktail tablet. Cells were lysed by sonication by short bursts until disrupted. Cells were spun at 15,000 g for 15 min at 4°C to pellet down cell debris. The supernatant was collected and ultra centrifuged at 40,000 g for 2 hrs. The supernatant was collected and passed through a 45 µm filter before loading into a Novagen His•Bind® column containing Ni^{2+}-charged His•Bind Resin. The protein was collected in 20 mM Tris-HCl (pH 7.9), 500 mM NaCl, and 1 M imidazole using His-bind kit protocol (Novagen). The protein containing fractions were immediately pooled. The dialysis was performed using 20 mM Tris-HCl (pH 7.6), 0.15 mM NaCl to remove imidazole from the protein preparation. The

samples were passed through a 0.22 µm filter (Millipore) before conducting the spectroscopy measurements. The concentration of purified protein was calculated using Bradford assay with as standard. The purified protein was then stored at -80°C for further studies.

2.2.2.4. Anisotropy Measurements

The protein- RNA interaction and protein complex- RNA interaction were studied using the change in anisotropy (*r*) of structurally different fluorescein labeled RNA. Twenty to fifty nM fluorescein labeled RNA was used during the titration with increasing concentrations of eIF4B or eIF4B▪eIF4A complex. The fluorophore was excited at 490 nm and emission was monitored at 519 nm. All titrations were carried out in titration buffer containing 20 mM HEPES, 100 mM KCl (pH 7.6) at 22 ºC. A Spex Fluorolog τ2 spectrofluorimeter equipped with excitation and emission polarizers was used. Anisotropy was measured using an L-format detection configuration. The excitation and emission slits were 4 nm and 5 nm, respectively. All samples were incubated for 10 min before data collection.

2.2.3. Results

2.2.3.1. RNA Sequences and Predicted Structures

RNAfold server from Vienna RNA package [94-96] was used to predict the minimum free energy secondary structure of various RNA sequences.

The first sequence was designed using a random sequence to give desired and stable stem-loop structure with some unpaired nucleotides on either end. This sequence has 4 base pair stem and 5 nucleotide loop. The other sequences were derived from this using minimum change in nucleotide composition to obtain the desired structures.

Three more sequences with different structures were designed. The second sequence we designed was linear RNA to answer the question whether the binding of eIF4B is low only with poly (A) RNA or with any linear RNA. Next, RNA with a 4 base pair stem and 8 nucleotide loop was used to see the effect of the size of the loop on binding. The fourth sequence used in this study was designed with a 5 base pair stem and completely base paired stem to understand if ds RNA is important for this interaction. All designed sequences used in this study were 29 nucleotide in length (Table 10).

S.No.	RNA Characterstics	RNA Sequence	RNA Structure
1.	20mer poly (A) oligonucleotide	5’AAAAAAAAAAAAAAAAAAAA3’	
2.	29mer RNA - 4 bp stem 5 nt loop with fluorescein label at 3' end.	5'GGGAAGGAAGGUCGAAAGGACCAACAGCU Flo 3'	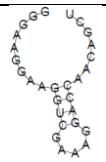
3.	29mer linear RNA with fluorescein label at 3' end	5' GGGAAGCAACGAGGAAGGGAUCAACAGUU Flo 3'	
4.	29mer RNA - 4 bp stem 8 nt loop, fluorescein label at 3' end	5’ GGGAUCGGAUGAAGCACCGGGUAAACAGC Flo 3'	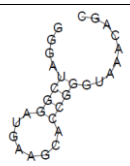
5.	29mer RNA- 5 nt loop and complete bp stem, fluorescein label at 3' end	5' GGGUAAGGAAGGCUGAACCUUCCUUACCC Flo 3'	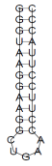
6.	Partially dsRNA fluorescein label at 5' end of smaller strand	5’GGGACCAUGGAACAACAUUAUCGCUGCGCUGCCCC 3' 3’GCGACGCGACGGGGFlo5’	

Table 10. ***Sequences and Predicted Structures of the RNA used for binding analysis with eIF4B***

2.2.3.2. Interaction of eIF4B with structurally different RNA

Initially in the absence of protein, low anisotropy was observed because of large amount of the tumbling motion in the relatively small RNA molecule. Upon addition of eIF4B to structurally different RNA, an increase in fluorescence anisotropy was observed. The increase in anisotropy indicates that the RNA is interacting with protein, resulting in less tumbling because of the bigger molecule now associated with it.

The equilibrium dissociation constant was calculated using the change in anisotropy as described in Material and Methods. The K_d for 29 mer linear RNA demonstrated the same pattern as observed for Poly (A) RNA in the previous part of this study with values of 57.5 ± 16.5 nM and 77.0 ± 7 nM, respectively.

More than 40 fold tighter binding (1.6 ± 0.5 nM) was observed for 29 mer RNA with a stem loop structure (5 nucleotide loop and 4 base pair stem) and some unpaired nucleotides on either end. 29mer RNA with 4 base pair stem and 8 nucleotide loop (Figure 19), 29mer RNA with 5 base pair stem and completely base paired stem and partially double stranded RNA were not much different in the binding interactions giving the following values; 6.9 ± 3.1 nM,7.7 ± 1.0 nM and 7.2 ± 0.7 nM, respectively (Table 11).

	RNA Structures	4B(1-527) (nM)
1.	Poly (A)	77.0 ± 7
2.	29mer RNA linear	57.5 ± 16.5
3.	29mer RNA 5nt loop 4nt stem	1.6 ± 0.5
4.	29mer RNA 8nt loop 4nt stem	6.9 ± 3.1
5.	29mer RNA 5nt loop and complete base paired stem	7.7 ± 1.0
6.	Partially double stranded RNA	7.2 ± 0.7

Table 11. ***Equilibrium dissociation constants for the interaction of eIF4B full length with structurally different 29mer RNA's, determined by fluorescence anisotropy.***

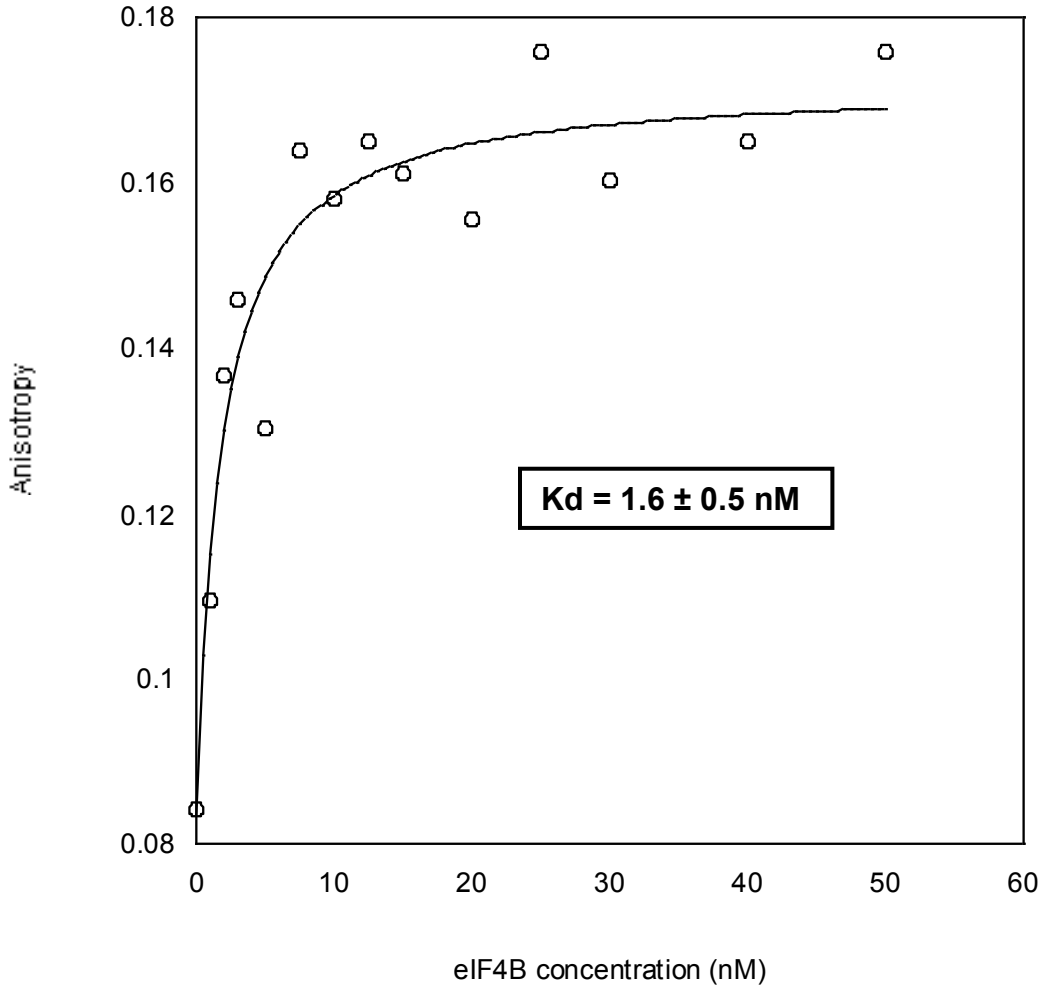

Figure 20. ***Fluorescence anisotropy measurements on binding of eIF4B full length with 29mer RNA with 4 basepair stem 5 nucleotide loop and fluorescein label at 3' end.***

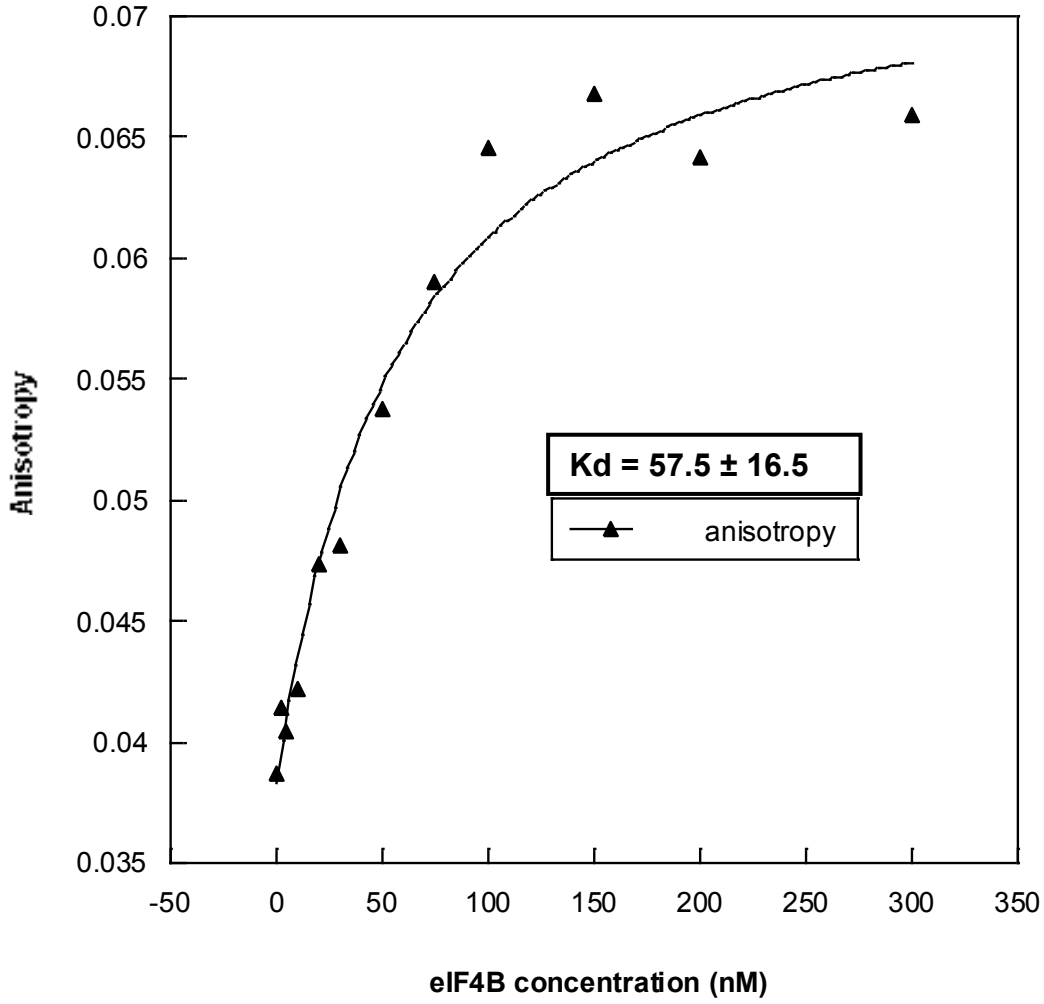

Figure 21. ***Fluorescence anisotropy measurements on binding of eIF4B full length with 29mer linear RNA and fluorescein label at 3' end.***

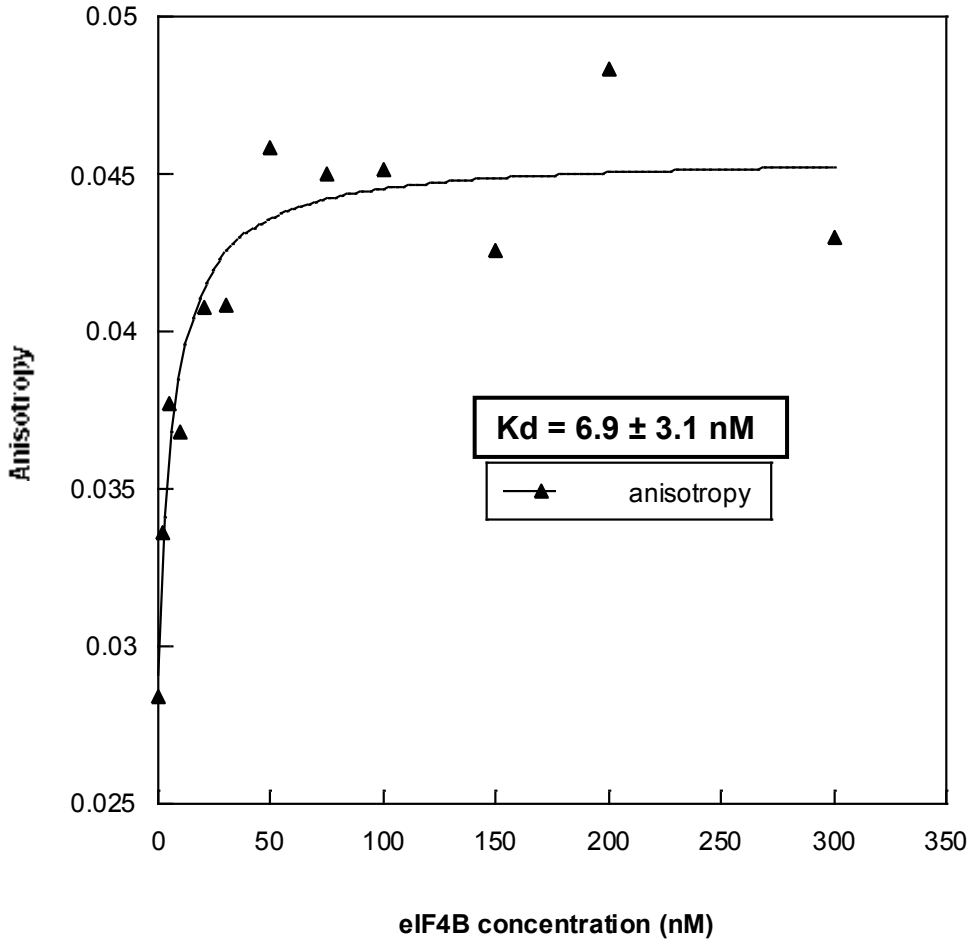

Figure 22. ***Fluorescence anisotropy measurements on binding of eIF4B full length with 29mer RNA with 8 nucleotide loop 4 basepair stem and fluorescein label at 3' end.***

2.2.3.3. Interaction of 320-527 eIF4B mutant and structurally different RNA

The fluorescence anisotropy was also used to study the binding of eIF4B (320-527) deletion mutant with poly (A) RNA, linear RNA and 29 mer RNA with stem loop structure (5 nucleotide loop and 4 base paired stem) and some unpaired nucleotides on either ends. The 320-527 mutant contains only the C-terminal RNA binding domain. The earlier part of this study had suggested that this is a critical domain affecting RNA binding.

Data analysis revealed that full length eIF4B and 320-527 deletion mutant show similar binding constants with structurally different RNA's. The binding was tighter with structured RNA as compared to the linear and poly (A) RNA. The 320-527 eIF4B mutant protein exhibits a K_d of 61.9 ± 6.4 nM with poly (A) RNA, 46.0 ± 8.4 nM with 29mer linear RNA and 3.6 ± 1.2 with the structured RNA (Table 12).

S. No.	RNA Structures	4B(1-527) (nM)	4B(320-527) (nM)
1	Poly (A)	77.0 ± 7	61.9 ± 6.4
2	29mer RNA linear	57.5 ± 16.5	46.0 ± 8.4
3	29mer RNA 5loop4stem	1.6 ± 0.5	3.6 ± 1.2

Table 12. ***Equilibrium dissociation constants for the interaction of eIF4B full length and 320-527 deletion mutant with structurally different 29mer RNA's.***

2.2.3.4. Interaction of EIF4A complexed with/without EIF4B and different RNA

To determine the effect of secondary structure on binding of RNA with eIF4A and eIF4B, we used fluorescein labeled RNA and titrated eIF4B and eIF4A alone and in complex. The fluorescence anisotropy studies were performed to calculate the dissociations constants as described in Material and Methods.

The complex of eIF4B and eIF4A was prepared by mixing eIF4B and eIF4A in 1:4 molar ratios as reported earlier to make sure that more than 95% of eIF4B is in complex and the binding that we observe with oligonucliotide comes from complex of proteins rather than any one protein.

The eIF4B was found to be binding very tightly with structured RNA as compared to linear and poly A RNA as described earlier. The eIF4A itself did not show much significant binding with RNA. When it was complexed with eIF4B, the binding was seen to be significantly increased but complex binding is significantly weaker as compared to eIF4B alone.

S. no.	RNA structure	eIF4A (nM)	eIF4A. eIF4B complex (nM)
1	29mer RNA 5loop4stem	Low binding	6.0 ± 2.4
2	29mer RNA linear		132.8 ± 60.7

Table 13. ***Equilibrium dissociation constants for the interaction of eIF4A alone and in complex with eIF4B full length with structurally different 29mer RNA's.***

2.2.4. Conclusions and Discussion

The secondary structure present in the 5' untranslated region of different mRNAs plays an important role in translation and regulation. The higher the amount of secondary structure in the mRNA, the more difficult it is for a ribosome to bind and scan for the initiation codon.

It was reported earlier that eIF4B enhances the binding affinity of eIF4A towards both RNA and ATP [46, 97, 98]. Furthermore, it has been observed that the eIF4B and eIF4H show more stimulation of eIF4A helicase activity as the stability of duplex increases [99]. EIF4B stimulates the eIF4A ability to unwind secondary structure with unpaired residues flanking the structure, as compared with a blunt end duplex [99]. It was also suggested that eIF4B binds the newly separated single strand and destabilizes the duplex substrate, thereby facilitating eIF4A unwinding of more residues in the single binding cycle[99]. Our results support these biochemical results. We also observed that the binding of eIF4B was very tight with RNA containing a stem loop structure and unpaired residues. This tight binding by eIF4B might assist eIF4A to interact longer with the mRNA and hence enable it to undergo more efficient helicase action and subsequent translation initiation. This is consistent with the observation by other groups that in yeast translation of mRNA with moderately stable secondary structure in 5' leader is highly stimulated by eIF4B as compared to mRNA with little secondary structure [2, 79]. Further, it's been observed by Shatsky et. al.[100], that *in vitro* in higher

eukaryotes eIF4B is required for 48S translation initiation complex assembly on mRNA with moderately stable secondary structure in the 5′ leader [2, 100]. Our results suggest eIF4B discrimination among structurally different mRNA is a significant factor in successful translation initiation.

We also found the eIF4A binds weakly with RNA alone as observed earlier but when it was complexed with the eIF4B, the binding of the complex became much tighter. This suggests that the stronger binding affinity of eIF4B with RNAs helps the eIF4A to stay longer on mRNA and hence promotes its helicase function and unwinding the longer stretches of mRNA before it dissociates from the complex. This results in a more efficient translation initiation process. It was reported that eIF4A has only a very weak helicase activity on its own [87] and cannot process because it dissociates from ssRNA faster than it hydrolyses ATP [81, 82, 85, 88]. The observation that eIF4A1 complexed with eIF4B or eIF4H bound to RNAs much longer than those bound by eIF4AI alone [101] supports our observation that eIF4B is stabilizing the interaction of eIF4A on mRNA for helicase activity to unwind the mRNA for ribosomal binding and scanning. This part of the study adds to our current understanding of the translation initiation process in mRNA's with different structural elements in their 5' untranslated region.

Appendix

1. Buffers and solutions used in experiments:

1.1. Media and solutions used in *E.coli* cell culture

1.1.1. LB media

NaCl	10g
Yeast extract	5g
Tryptone	10g
DDH_2O	1000ml
Total volume	1 Liter

1.1.2. Antibiotic stock solutions

a) 100 mg/ml Ampicillin

1.0 g Ampicillin in 10 ml DD H_2O

b) 34 mg/ml Choramphenicol

0.34 g in 10 ml of 100% ethanol

1.2. Buffers for Protein Purification

1.2.1. Buffers for GST tag protein purification

1.2.1.1. Binding buffer (1X PBS)

140 mM NaCl

2.7 mM KCl

10 mM Na_2HPO_4

1.8 mM KH_2PO_4

pH 7.4

1.2.1.2. Elution buffer

50 mM Tris – HCl

10mM Reduced Glutathione

pH 8.0

1.2.2. Buffers for His tag protein purification

1.2.2.1. Binding buffer

0.5 M NaCl

20 mM Tris – HCl

5 mM Imidazole

pH 7.9

1.2.2.2. Wash buffer

0.5 M NaCl

60 mM Imidazole

20 mM Tris – HCl

pH 7.9

1.2.2.3. Elution buffer

1 M Imidazole

0.5 M NaCl

20 mM Tris – HCl

pH 7.9

1.2.2.4. Strip buffer

0.5 M NaCl

100 mM EDTA

20 mM Tris – HCl

pH 7.9

1.2.2.5. Charge buffer

50 mM $NiS0_4$

1.3. Buffers for SDS Polyacrylamide Gel Electrophoresis

1.3.1. Monomer solution

30.8 % of acrylamide

2.7 % of N,N'-methylene bis-acrylamide

1.3.2. 4X Running gel buffer

1.5 M Tris-Cl

pH 8.8

1.3.3. 4X Stacking gel buffer

0.5 M Tris-Cl

pH 6.8

1.3.4. 10 % SDS and 10 % Ammonium persulphate

1.3.5. 2X Treatment buffer

0.125 M Tris-Cl

4.0 % SDS

20 % v/v Glycerol

0.2 M DTT

0.02 % Bromophenol blue

pH 6.8

1.3.6. Tank buffer

0.025 Tris

0.192 M Glycine

0.1 % SDS

pH 8.3

2. Protein Quantitation by the Bradford Method

The Coomassie Plus (Bradford) assay was used to determine the protein concentration.

Coomassie dye, present in the assay reagent, binds with the protein in acidic medium, forming a blue color complex that is measured at 595nm.

Preparation of diluted BSA standards: A fresh set of protein standards were prepared by diluting the 2.0 mg/ml BSA stock standard preferably in the same diluents as of protein.

Table: Preparation of the Diluted BSA Standards

Vial	Volume of Diluent	Volume of the BSA to Add	Final BSA Concentration
A.	0 µl	300 µl of (Stock)	2000 µg/ml
B.	125 µl	375 µl of (Stock)	1500 µg/ml
C.	325 µl	325 µl of (Stock)	1000 µg/ml
D.	175 µl	175 µl of (B)	750 µg/ml
E.	325 µl	325µl of (C)	500 µg/ml
F.	325 µl	325 µl of (E)	250 µg/ml
G.	325 µl	325 µl of (F)	125 µg/ml
H.	400 µl	100 µl of (G)	25 µg/ml
I.	400 µl	0	0 µg/ml (Blank)

Assay: Prior to assay the Coomassie® Plus reagent is equilibrated to room temperature and is gently mixed several times by inverting the bottle. 0.05 ml of each standard or unknown sample is added into labeled UV cuvette. 0.05 ml of the diluent is used for the blank. 1.5 ml of the Coomassie® Plus Reagent is added to each tube and mixed well.

The absorbance of the reaction mixture is measured on a UV/Vis spectrophotometer at 595 nm. First the absorbance of the blank is measure at 595 nm and spectrophotometer reading is brought to zero. The absorbance for the remaining cuvettes is then measured at 595 nm. The standard curve is drawn by plotting the average blank corrected 595 nm reading for each BSA standard versus its concentration in µg/ml. Using the standard curve, the protein concentration for each unknown sample is determined.

3. SDS Polyacrylamide Gel Electrophoresis (SDS-PAGE)

Assembling gel apparatus*:* The gel electrophoresis equipment was assembled according to the apparatus manual provided by manufacturer.

The gels were prepared using the buffers and reagents listed in Appendix 1.3. The gel was cast using the following protocol.

Resolving gel:

Gel concentration of 12.5%.

Reagents	Volume (To make15 ml)
Monomer solution	6.25 ml
4X Running gel buffer	3.75 ml
10% SDS	0.15 ml
ddH_2O	4.775 ml
10% Ammonium persulphate	75 µl
TEMED (added last)	5 µl

Mix ingredients very carefully in the order shown above, ensuring no air bubbles form. Pour into glass plate assembly. Overlay gel with isopropanol to ensure a flat surface and to exclude air. Wash off isopropanol with water after gel has polymerized (about15 min).

Stacking Gels:

Gel concentration of 4%.

Reagents	Volume (To make 5 ml)
Monomer solution	0.665 ml
4X Stacking gel buffer	1.25 ml
10% SDS	0.05 ml
ddH_2O	3.0 ml
10% Ammonium persulphate	25 µl
TEMED (added last)	2.5 µl

Mix as before, then pour onto top of set resolving gel, insert comb, allow to polymerize (about 30 minutes), remove comb, fill with electrophoresis buffer. Assemble top tank onto glass plate assembly. Fill with electrophoresis buffer.

Electrophoresis buffer: The final tank buffer composition is 0.025 M Tris-HCl, 192 M glycine, 0.1% SDS, pH 8.3, made by diluting a 10x stock solution. This goes in both top and bottom tanks.

Protein samples: Protein samples were prepared by mixing supernatant and 50µL 1:1 (v:v) with SDS-PAGE 2X treatment buffer. For liquid / purified samples, take e.g. 100 µL and add 50 - 100 µL of disruption mix. Eppendorf tubes containing the samples are heated for 5 min at boiling water in a "float" in a water bath then sat on ice for 10 minutes. Layer samples under buffer into wells on stacking gels. Connect up apparatus to the power supply to begin electrophoresis. Set voltage as 150V and current as 20mA.

Staining the gel: Stain the gel by using Coomassie Brilliant Blue R250. Make up stain: 0.2% Coomassie Brilliant Blue R250 in 45% 45% 10 % methanol water acetic acid. Cover gel with staining solution, seal in plastic box and leave overnight on shaker (RT) or for 2 to 3 hours at 37 ºC also with agitation.

Destaining the gel : Destain with 25% 65% 10% methanol water acetic acid mix, with agitation. Change the distaining solution several times until the gel background color is transparent.

Bibliography

1. Lou H, C.Y., LaVoy JE, Major ME, Hagedorn CH. , *Analysis of mutant NS5B proteins encoded by isolates from chimpanzees chronically infected following clonal HCV RNA inoculation.* Virology, 2003. **317**(1): p. 65-72.

2. Cheng, S. and D.R. Gallie, *Wheat eukaryotic initiation factor 4B organizes assembly of RNA and eIFiso4G, eIF4A, and poly(A)-binding protein.* J Biol Chem, 2006. **281**(34): p. 24351-64.

3. Cheng, S., Sultana, Shemaila, Goss, Dixie J., Gallie, Daniel R., *Translation Initiation Factor 4B Homodimerization, RNA Binding, and Interaction with Poly(A)-binding Protein Are Enhanced by Zinc.* J. Biol. Chem., 2008. **283**(52): p. 36140-36153.

4. Lakowicz, J.R., *Principles of Fluorescence Spectroscopy*. 4 ed. 2006: Springer. 954.

5. Alter, H.J., *To C or not to C: these are the questions.* Blood, 1995. **85**(7): p. 1681-95.

6. *NIH Consensus Statement on Management of Hepatitis C: 2002.* NIH Consens State Sci Statements, 2002. **19**(3): p. 1-46.

7. Sarbah, S.A. and Z.M. Younossi, *Hepatitis C: an update on the silent epidemic.* J Clin Gastroenterol, 2000. **30**(2): p. 125-43.

8. Choo, Q.L., Kuo, G., Weiner, A.J., Overby, L.R., Bradley, D.W., and Houghton, M. , *Isolation of a cDNA clone derived from a blood-borne non-A, non-B viral hepatitis genome.* Science, 1989. **244**(4902): p. 359-62.

9. Saito, I., Miyamura, T., Ohbayashi, A., Harada, H., Katayama, T., Kikuchi, S., Watanabe, Y., Koi, S., Onji, M., and Ohta, Y., *Hepatitis C virus infection is associated with the development of hepatocellular carcinoma.* Proc Natl Acad Sci U S A, 1990. **87**(17): p. 6547-9.

10. Rehermann, B., Chang, K. M., McHutchinson, J., Kokka, R., Houghton, M., Rice, C. M., and Chisari, F. V., *Differential cytotoxic T-lymphocyte responsiveness to the hepatitis B and C viruses in chronically infected patients.* J Virol, 1996. **70**(10): p. 7092-102.

11. Bougie, I., S. Charpentier, and M. Bisaillon, *Characterization of the metal ion binding properties of the hepatitis C virus RNA polymerase.* J Biol Chem, 2003. **278**(6): p. 3868-75.

12. Bressanelli S, T.L., Rey F A, Francesco R D, *Structural analysis of the Hepatitis C virus RNA polymerase in complex with Ribonucleotides.* J Virol, 2002. **76**(7): p. 3482-92.

13. Foy E, L.K., Wang C, Sumpter R, Jr., Ikeda M, Lemon S M, Gale M., Jr., , *Regulation of interferon regulatory factor-3 by the hepatitis C virus serine protease. .* Science, 2003. **300**: p. 1145-1148.

14. Forns, X., R.H. Purcell, and J. Bukh, *Quasispecies in viral persistence and pathogenesis of hepatitis C virus.* Trends in Microbiology, 1999. **7**(10): p. 402-410.

15. Forns, X., J. Bukh, and R.H. Purcell, *The challenge of developing a vaccine against hepatitis C virus.* Journal of Hepatology, 2002. **37**(5): p. 684-695.

16. Koonin E V, *A common set of conserved motifs in a vast variety of putative nucleic acid-dependent ATPases including MCM proteins involved in the initiation of eukaryotic DNA replication.* Nucleic Acids Res, 1993. **21**(11): p. 2541-7.

17. Behrens SE, T.L., De Francesco R., *Identification and properties of the RNA-dependent RNA polymerase of hepatitis C virus.* EMBO J, 1996. **15**(1): p. 12-22.

18. Lohmann V, K.F., Herian U, Bartenschlager R., *Biochemical properties of hepatitis C virus NS5B RNA-dependent RNA polymerase and identification of amino acid sequence motifs essential for enzymatic activity.* J Virol, 1997. **71**(11): p. 8416-28.

19. O'Reilly EK, K.C., *Analysis of RNA-dependent RNA polymerase structure and function as guided by known polymerase structures and computer predictions of secondary structure.* Virology, 1998. **252**(2): p. 287-303.

20. Oh JW, I.T., Lai MM., *A recombinant hepatitis C virus RNA-dependent RNA polymerase capable of copying the full-length viral RNA.* J virol, 1999. **73**(9): p. 7694-702.

21. Vo NV, T.J., Lai MM, *Enzymatic characterization of the full-length and C-terminally truncated hepatitis C virus RNA polymerases: function of the last 21 amino acids of the C terminus in template binding and RNA synthesis.* Biochemistry, 2004. **43**(32): p. 10579-91.

22. Zhong, W., Uss, A. S., Ferrari, E., Lau, J. Y. N., and Hong, Z. , *De novo initiation of RNA synthesis by hepatitis C virus nonstructural protein 5B polymerase.* J. Virol. , 2000. **74**: p. 2017-2022.

23. Carroll, S.S., Sardana, V., Yang, Z., Jacobs, A. R., Mizenko, C., Hall, D., Hill, L., Zugay-Murphy, J., and Kuo, L. C. , *Only a small fraction of purified hepatitis C RNA-dependent RNA polymerase is catalytically competent: implications for viral replication and in vitro assays.* Biochemistry, 2000. **39**: p. 8243-8249.

24. Ferrari, E., Wright-Mnogue, J., Fang, J.W., Baroudy, B.M., Lau, J.Y., and Hong, Z., *Characterization of soluble hepatitis C virus RNA-dependent RNA polymerase expressed in Escherichia coli.* Journal of Virology 1999. **73**: p. 1649-1654.

25. Cheney, I.W., Naim, S., Lai, V. C. H., Dempsey, S., Bellows, D., Walker, M. P., Shim, J. H., Horscroft, N., Hong, Z., and Zhong, W., *Mutations in NS5B polymerase of hepatitis C virus: impacts on in vitro enzymatic activity and viral RNA replication in the subgenomic replicon cell culture.* Virology, 2002. **297**: p. 298-306.

26. Sun, X.L., Johnson, R. B., Hockman, M. A., and Wang, Q. M. , *De novo RNA synthesis catalyzed by HCV RNA-dependent RNA polymerase.* Biochem. Biophys. Res. Commun. , 2000. **268**: p. 798-803.

27. Uchiyama, Y., Huang, Y., Kanamori, H., Uchida, M., Doi, T., Takamizawa, A., Hamakubo, T., and Kodama, T. , *Measurement of HCV RdRp activity with C-terminal 21 aa truncated NS5b protein: optimization of assay conditions.* Hepatol. Res. , 2002. **23**: p. 90-97.

28. Tomei, L., Vitale, R. L., Iccitti, I., Serafini, S., Altamura, S., Vitelli, A., and De Francesco, R., *Biochemical characterization of a hepatitis C virus RNA-dependent RNA polymerase mutant lacking the C-terminal hydrophobic sequence.* J. Gen. Virol. , 2000. **81**: p. 759-767.

29. Yamashita, T., Kaneko, S., Shirota, Y., Qin, W., Nomura, T., Kobayashi, K., and Murakami, S. , *RNA-dependent RNA polymerase activity of the soluble recombinant hepatitis C virus NS5B protein truncated at the C-terminal region.* J. Biol. Chem.
, 1998. **273**: p. 15479-15486.

30. Luo, G., Hamatake, R. K., Mathis, D. M., Racela, J., Rigat, K. L., Lemm, J., and Colonno, R. J. , *De novo initiation of RNA synthesis by the RNA-dependent RNA polymerase (NS5B) of hepatitis C virus.* J. Virol. , 2000. **74**: p. 851-863.

31. Johnson, R.B., Sun, X. L., Hockman, M. A., Villarreal, E. C., Wakulchik, M., and Wang, Q. M. , *Specificity and mechanism analysis of hepatitis C virus RNA-dependent RNA polymerase.* Arch. Biochem. Biophys., 2000. **377**: p. 129-134.

32. Bressanelli, S., et al., *Crystal structure of the RNA-dependent RNA polymerase of hepatitis C virus.* Proc Natl Acad Sci U S A, 1999. **96**(23): p. 13034-9.

33. Lesburg, C.A., et al., *Crystal structure of the RNA-dependent RNA polymerase from hepatitis C virus reveals a fully encircled active site.* Nat Struct Biol, 1999. **6**(10): p. 937-43.

34. Bressanelli, S., et al., *Structural Analysis of the Hepatitis C Virus RNA Polymerase in Complex with Ribonucleotides.* J. Virol., 2002. **76**(7): p. 3482-3492.

35. De Francesco, R., et al., *Approaching a new era for hepatitis C virus therapy: inhibitors of the NS3-4A serine protease and the NS5B RNA-dependent RNA polymerase.* Antiviral Research, 2003. **58**(1): p. 1-16.

36. Invitrogen, *Molecular Probes: The Handbook.*

37. C.T.Ranjith-Kumar, e.a., *Mechanism of denovo initiatio by the Hepatitis C Virus RNA dependent RNA polymerase: Role of divalent metals.* J.Virol, 2002. **76**(24): p. 12513-12525.

38. Gottesfeld, J.M., Belitsky, J. M., Melander, C., Dervan, P. B., and Luger, K., *Blocking transcription through a nucleosome with synthetic DNA ligands.* J. Mol. Biol. , 2002. **321**: p. 249–263.

39. Bougie I, C.S., Bisaillon M, *Characterization of the metal ion binding properties of the hepatitis C virus RNA polymerase.* J Biol Chem, 2003. **278**(6): p. 3868-75.

40. Kashiwagi, T., Hara,K., Kohara,M., Iwahashi,J., Hamada,N., Honda-Yoshino,H.,Toyoda,T., *Promoter/origin structure of the complementary strand of hepatitis C virus genome.* J. Biol. Chem. , 2002. **277**: p. 28700-28705

41. Schuster, C., Isel,C., Imbert, I., Ehresmann,C., Marquet,R., Kieny, M.P., *Secondary structure of the 3' terminus of hepatitis C virus minus-strand RNA.* J. Virol., 2002. **76**: p. 8058-8068.

42. Astier-Gin, T., Bellecave, P., Litvak, S., and Ventura, M., *Template requirements and binding of hepatitis C virus NS5B polymerase during in vitro RNA synthesis from the 3'-end of virus minus-strand RNA.* FEBS Journal, 2005. **272**(15): p. 3872-3886.

43. Farci, P., *Hepatitis C virus. The importance of viral heterogeneity.* Clin Liver Dis, 2001. **5**(4): p. 895-916.

44. Ogata, N., Alter, H. J., Miller, R. H., and Purcell, R. H., *Nucleotide sequence and mutation rate of the H strain of hepatitis C virus.* Proc. Natl Acad Sci (USA), 1991. **88**(8): p. 3392-3396.

45. Ludmerer, S.W., et al., *Replication Fitness and NS5B Drug Sensitivity of Diverse Hepatitis C Virus Isolates Characterized by Using a Transient Replication Assay.* Antimicrob. Agents Chemother., 2005. **49**(5): p. 2059-2069.

46. Bi, X., J. Ren, and D.J. Goss, *Wheat germ translation initiation factor eIF4B affects eIF4A and eIFiso4F helicase activity by increasing the ATP binding affinity of eIF4A.* Biochemistry, 2000. **39**(19): p. 5758-65.

47. Preiss, T. and W.H. M, *Starting the protein synthesis machine: eukaryotic translation initiation.* Bioessays, 2003. **25**(12): p. 1201-11.

48. Sonenberg, N. and A.G. Hinnebusch, *Regulation of Translation Initiation in Eukaryotes: Mechanisms and Biological Targets.* 2009. **136**(4): p. 731-745.

49. Merrick, W.C., *Eukaryotic protein synthesis: an in vitro analysis.* Biochimie, 1994. **76**(9): p. 822-30.

50. Merrick, W.C. and J.W.B. Hershey, *The Pathway and Mechanism of Eukaryotic Protein Synthesis*. 1996: Cold Spring Harbor Laboratory, Painview, NY. pp 31-69.

51. Browning, K.S., Fletcher, L., Lax, S. R., and Ravel, J. M., *Evidence that the 59-kDa protein synthesis initiation factor from wheat germ is functionally similar to the 80-kDa initiation factor 4B from mammalian cells.* Journal of Biological Chemistry, 1989. **264**(15): p. 8491-8494.

52. Metz, A.M., Wong, K. C., Malmstrom, S. A., and Browning, K. S., *Eukaryotic initiation factor 4B from wheat and Arabidopsis thaliana is a member of a multigene family.* Biochem Biophys Res Commun, 1999. **266**(2): p. 314-21.

53. Bi, X. and D.J. Goss, *Wheat germ poly(A)-binding protein increases the ATPase and the RNA helicase activity of translation initiation factors eIF4A, eIF4B, and eIF-iso4F.* J Biol Chem, 2000. **275**(23): p. 17740-6.

54. Vornlocher, H.P., Hanachi, P., Ribeiro, S., and Hershey, J. W., *A 110-kilodalton subunit of translation initiation factor eIF3 and an associated 135-kilodalton protein are encoded by the Saccharomyces cerevisiae TIF32 and TIF31 genes.* J Biol Chem, 1999. **274**(24): p. 16802-12.

55. Methot, N., M.S. Song, and N. Sonenberg, *A region rich in aspartic acid, arginine, tyrosine, and glycine (DRYG) mediates eukaryotic initiation factor 4B (eIF4B) self-association and interaction with eIF3.* Mol Cell Biol, 1996. **16**(10): p. 5328-34.

56. Van Der Kelen, K., Beyaert, R., Inze, D., and De Veylder, L., *Translational control of eukaryotic gene expression.* Crit Rev Biochem Mol Biol, 2009. **44**(4): p. 143-68.

57. Trachsel, H., Erni, B., Schreier, M. H., and Staehelin, T., *Initiation of mammalian protein synthesis : II. The assembly of the initiation complex with purified initiation factors.* J Mol Biol, 1977. **116**(4): p. 755-767.

58. Benne, R. and J.W. Hershey, *The mechanism of action of protein synthesis initiation factors from rabbit reticulocytes.* Journal of Biological Chemistry, 1978. **253**(9): p. 3078-3087.

59. Pestova, T., C. Hellen, and I. Shatsky, *Canonical eukaryotic initiation factors determine initiation of translation by internal ribosomal entry.* Mol. Cell. Biol., 1996. **16**(12): p. 6859-6869.

60. Morino, S., Imataka, H., Svitkin, Y. V., Pestova, T. V., and Sonenberg, N., *Eukaryotic Translation Initiation Factor 4E (eIF4E) Binding Site and the Middle One-Third of eIF4GI Constitute the Core Domain for Cap-Dependent Translation, and the C-Terminal One-Third Functions as a Modulatory Region.* Mol. Cell. Biol., 2000. **20**(2): p. 468-477.

61. Altmann, M., Wittmer, B., Methot, N., Sonenberg, N., and Trachsel, H., *The Saccharomyces cerevisiae translation initiation factor Tif3 and its mammalian homologue, eIF-4B, have RNA annealing activity.* EMBO J, 1995. **14**(15): p. 3820-7.

62. Le, H., Tanguay, R. L., Balasta, M. L., Wei, C. C., Browning, K. S., Metz, A. M., Goss, D. J., and Gallie, D. R., *Translation initiation factors eIF-iso4G and eIF-4B interact with the poly(A)-binding protein and increase its RNA binding activity.* J Biol Chem, 1997. **272**(26): p. 16247-55.

63. Le, H., K.S. Browning, and D.R. Gallie, *The phosphorylation state of poly(A)-binding protein specifies its binding to poly(A) RNA and its interaction with eukaryotic initiation factor (eIF) 4F, eIFiso4F, and eIF4B.* J Biol Chem, 2000. **275**(23): p. 17452-62.

64. Bushell, M., Wood, W., Carpenter, G., Pain, V. M., Morley, S. J., and Clemens, M. J., *Disruption of the Interaction of Mammalian Protein Synthesis Eukaryotic Initiation Factor 4B with the Poly(A)-binding Protein by Caspase- and Viral Protease-mediated Cleavages.* J Biol Chem, 2001. **276**(26): p. 23922-23928.

65. Wei, C.C., Balasta, M. L., Ren, J., and Goss, D. J., *Wheat germ poly(A) binding protein enhances the binding affinity of eukaryotic initiation factor 4F and (iso)4F for cap analogues.* Biochemistry, 1998. **37**(7): p. 1910-6.

66. Khan, M.A. and D.J. Goss, *Translation initiation factor (eIF) 4B affects the rates of binding of the mRNA m7G cap analogue to wheat germ eIFiso4F and eIFiso4F.PABP.* Biochemistry, 2005. **44**(11): p. 4510-6.

67. Wells, S.E., et al., *Circularization of mRNA by eukaryotic translation initiation factors.* Mol Cell, 1998. **2**(1): p. 135-40.

68. Kelly, S.M. and N.C. Price, *The use of circular dichroism in the investigation of protein structure and function.* Current Protein & Peptide Science, 2000. **1**(4): p. 349-384.

69. Ranjbar, B. and P. Gill, *Circular Dichroism Techniques: Biomolecular and Nanostructural Analyses- A Review.* Chemical Biology & Drug Design, 2009. **74**(2): p. 101-120.

70. Hong, J., Krishnamurthi, K., Zheng, W., and Sandberg, K., *In Vitro Translation of the Angiotensin AT1 Receptor in Wheat-Germ Extracts*. 2000. p. 171-192.

71. Matthews, J.A. and R.A. McKee, *In Vitro Protein Synthesis*. 1986. p. 131-147.

72. Olliver, L., A. Grobler-Rabie, and C.D. Boyd, *In Vitro Translation of mRNA in a Wheat Germ Extract Cell-Free System*. 2000. p. 891-894.

73. Luker, K.E. and G.D. Luker, *Applications of bioluminescence imaging to antiviral research and therapy: multiple luciferase enzymes and quantitation.* Antiviral Res, 2008. **78**(3): p. 179-87.

74. Khan, M.A. and D.J. Goss, *Phosphorylation states of translational initiation factors affect mRNA cap binding in wheat.* Biochemistry, 2004. **43**(28): p. 9092-7.

75. Anderson, C.W., J.W. Straus, and B.S. Dudock, *Preparation of a cell-free protein-synthesizing system from wheat germ.* Methods Enzymol, 1983. **101**: p. 635-44.

76. Rost, B., G. Yachdav, and J. Liu, *The PredictProtein server.* Nucleic Acids Res, 2004. **32**(Web Server issue): p. W321-6.

77. Porath, J., Carlsson, J., Olsson, I., and Belfrage, G., *Metal chelate affinity chromatography, a new approach to protein fractionation.* Nature, 1975. **258**(5536): p. 598-9.

78. Porath, J., *IMAC--Immobilized metal ion affinity based chromatography.* TrAC Trends in Analytical Chemistry, 1988. **7**(7): p. 254-259.

79. Altmann, M., Muller, P. P., Wittmer, B., Ruchti, F., Lanker, S., and Trachsel, H., *A Saccharomyces cerevisiae homologue of mammalian translation initiation factor 4B contributes to RNA helicase activity.* EMBO J, 1993. **12**(10): p. 3997-4003.

80. Methot, N., Pickett, G., Keene, J. D., and Sonenberg, N., *In vitro RNA selection identifies RNA ligands that specifically bind to eukaryotic translation initiation factor 4B: the role of the RNA remotif.* RNA, 1996. **2**(1): p. 38-50.

81. Lorsch, J.R. and D. Herschlag, *The DEAD box protein eIF4A. 1. A minimal kinetic and thermodynamic framework reveals coupled binding of RNA and nucleotide.* Biochemistry, 1998. **37**(8): p. 2180-93.

82. Pestova, T.V. and C.U. Hellen, *The structure and function of initiation factors in eukaryotic protein synthesis.* Cell Mol Life Sci, 2000. **57**(4): p. 651-74.

83. Rozen, F., Edery, I., Meerovitch, K., Dever, T. E., Merrick, W. C., and Sonenberg, N., *Bidirectional RNA helicase activity of eucaryotic translation initiation factors 4A and 4F.* Mol Cell Biol, 1990. **10**(3): p. 1134-44.

84. Jaramillo, M., Dever, T. E., Merrick, W. C., and Sonenberg, N., *RNA unwinding in translation: assembly of helicase complex intermediates comprising eukaryotic initiation factors eIF-4F and eIF-4B.* Mol Cell Biol, 1991. **11**(12): p. 5992-7.

85. Rogers, G.W., Jr., N.J. Richter, and W.C. Merrick, *Biochemical and kinetic characterization of the RNA helicase activity of eukaryotic initiation factor 4A.* J Biol Chem, 1999. **274**(18): p. 12236-44.

86. Linder, P., Lasko, P. F., Ashburner, M., Leroy, P., Nielsen, P. J., Nishi, K., Schnier, J., and Slonimski, P. P., *Birth of the D-E-A-D box.* Nature, 1989. **337**(6203): p. 121-2.

87. Rogers, G.W., N.J. Richter, and W.C. Merrick, *Biochemical and Kinetic Characterization of the RNA Helicase Activity of Eukaryotic Initiation Factor 4A.* Journal of Biological Chemistry, 1999. **274**(18): p. 12236-12244.

88. Lorsch, J.R. and D. Herschlag, *The DEAD box protein eIF4A. 2. A cycle of nucleotide and RNA-dependent conformational changes.* Biochemistry, 1998. **37**(8): p. 2194-206.

89. Yoder-Hill, J., Pause, A., Sonenberg, N., and Merrick, W. C., *The p46 subunit of eukaryotic initiation factor (eIF)-4F exchanges with eIF-4A.* J Biol Chem, 1993. **268**(8): p. 5566-73.

90. Imataka, H. and N. Sonenberg, *Human eukaryotic translation initiation factor 4G (eIF4G) possesses two separate and independent binding sites for eIF4A.* Mol Cell Biol, 1997. **17**(12): p. 6940-7.

91. Neff, C.L. and A.B. Sachs, *Eukaryotic translation initiation factors 4G and 4A from Saccharomyces cerevisiae interact physically and functionally.* Mol Cell Biol, 1999. **19**(8): p. 5557-64.

92. Khan, M.A., Yumak, H., Gallie, D. R., and Goss, D. J., *Effects of poly(A)-binding protein on the interactions of translation initiation factor eIF4F and eIF4F·4B with internal ribosome entry site (IRES) of tobacco etch virus RNA.* Biochimica et Biophysica Acta (BBA) - Gene Regulatory Mechanisms, 2008. **1779**(10): p. 622-627.

93. Kohler, J.J. and A. Schepartz, *Kinetic Studies of Fos.Jun.DNA Complex Formation: DNA Binding Prior to Dimerization†.* Biochemistry, 2000. **40**(1): p. 130-142.

94. Gruber, A.R., Lorenz, R., Bernhart, S. H., Neubock, R., and Hofacker, I. L., *The Vienna RNA websuite.* Nucleic Acids Res, 2008. **36**(Web Server issue): p. W70-4.

95. Hofacker, I.L., Fontana, W., Stadler, P. F., Bonhoeffer, L. S., Tacker, M., and Schuster, P., *Fast folding and comparison of RNA secondary structures.* Monatshefte für Chemie / Chemical Monthly, 1994. **125**(2): p. 167-188.

96. Mathews, D.H., Sabina, J., Zuker, M., and Turner, D. H., *Expanded sequence dependence of thermodynamic parameters improves prediction of RNA secondary structure.* J Mol Biol, 1999. **288**(5): p. 911-40.

97. Abramson, R.D., et al., *The ATP-dependent interaction of eukaryotic initiation factors with mRNA.* J Biol Chem, 1987. **262**(8): p. 3826-32.

98. Abramson, R.D., Dever, T. E., and Merrick, W. C., *Biochemical evidence supporting a mechanism for cap-independent and internal initiation of eukaryotic mRNA.* J Biol Chem, 1988. **263**(13): p. 6016-9.

99. Rogers, G.W., Jr., Richter, N. J., Lima, W. F., and Merrick, W. C., *Modulation of the Helicase Activity of eIF4A by eIF4B, eIF4H, and eIF4F.* J Biol Chem, 2001. **276**(33): p. 30914-30922.

100. Dmitriev, S.E., Terenin, I. M., Dunaevsky, Y. E., Merrick, W. C., and Shatsky, I. N., *Assembly of 48S Translation Initiation Complexes from Purified Components with mRNAs That Have Some Base Pairing within Their 5' Untranslated Regions.* Mol Cell Biol, 2003. **23**(24): p. 8925-8933.

101. Rozovsky, N., A.C. Butterworth, and M.J. Moore, *Interactions between eIF4AI and its accessory factors eIF4B and eIF4H.* RNA, 2008. **14**(10): p. 2136-48.